Counteracting Contributions of the Upper and Lower Meridional Overturning Limbs to the North Atlantic Nutrient Budgets: Enhanced Imbalance in 2010

L. Carracedo, H. Mercier, E. Mcdonagh, G. Rosón, R. Sanders, C. Moore, S. Torres-valdés, P. Brown, P. Lherminier, F. Pérez

Global Biogeochemical Cycles

RESEARCH ARTICLE
10.1029/2020GB006898

Key Points:

- The overturning circulation lower limb drives a net southward transport of oxygen and nutrients from the North to the South Atlantic
- Anomalous circulation in 2010 enhanced nutrient convergence by the overturning upper limb, boosting North Atlantic biological CO_2 uptake
- We observed a deep silicate divergence in the North Atlantic in 2004 and 2010 compatible with a transient response to reduced overturning

Supporting Information:

Supporting Information may be found in the online version of this article.

Correspondence to:

L. I. Carracedo,
lidia.carracedo@ifremer.fr,

Citation:

Carracedo, L. I., Mercier, H., McDonagh, E., Rosón, G., Sanders, R., Moore, C. M., et al. (2021). Counteracting contributions of the upper and lower meridional overturning limbs to the North Atlantic nutrient budgets: Enhanced imbalance in 2010. *Global Biogeochemical Cycles*, *35*, e2020GB006898. https://doi.org/10.1029/2020GB006898

Received 1 DEC 2020
Accepted 2 APR 2021

Counteracting Contributions of the Upper and Lower Meridional Overturning Limbs to the North Atlantic Nutrient Budgets: Enhanced Imbalance in 2010

L. I. Carracedo[1,2], H. Mercier[1], E. McDonagh[2,3], G. Rosón[4], R. Sanders[2,3], C. M. Moore[5], S. Torres-Valdés[6], P. Brown[2], P. Lherminier[1], and F. F. Pérez[7]

[1]University of Brest, CNRS, Ifremer, IRD, Laboratoire d'Océanographie Physique et Spatiale (LOPS), IUEM, Centre Ifremer de Bretagne, Plouzané, France, [2]National Oceanography Center (NOC), Southampton, UK, [3]NORCE Norwegian Research Centre, Bjerknes Centre for Climate Research, Bergen, Norway, [4]Faculty of Marine Sciences, University of Vigo, Campus Lagoas-Marcosende, Vigo, Spain, [5]School of Ocean and Earth Science, National Oceanography Centre, University of Southampton, Southampton, UK, [6]Alfred Wegener Institute, Am Handelshafen 12, Bremerhaven, Germany, [7]Instituto de Investigaciones Marinas, CSIC, Vigo, Spain

Abstract The North Atlantic Basin is a major sink for atmospheric carbon dioxide (CO_2) due in part to the extensive plankton blooms which form there supported by nutrients supplied by the three-dimensional ocean circulation. Hence, changes in ocean circulation and/or stratification may influence primary production and biological carbon export. In this study, we assess this possibility by evaluating inorganic nutrient budgets for 2004 and 2010 in the North Atlantic based on observations from the transatlantic A05-24.5°N and the Greenland-Portugal OVIDE hydrographic sections, to which we applied a box inverse model to solve the circulation and estimate the across-section nutrient transports. Full water column nutrient budgets were split into upper and lower meridional overturning circulation (MOC) limbs. According to our results, anomalous circulation in early 2010, linked to extreme negative NAO conditions, led to an enhanced northward advection of more nutrient-rich waters by the upper overturning limb, which resulted in a significant nitrate and phosphate convergence north of 24.5°N. Combined with heaving of the isopycnals, this anomalous circulation event in 2010 favored an enhancement of the nutrient consumption (5.7 ± 4.1 kmol-P s^{-1}) and associated biological CO_2 uptake (0.25 ± 0.18 Pg-C yr^{-1}, upper-bound estimate), which represents a 50% of the mean annual sea–air CO_2 flux in the region. Our results also suggest a transient state of deep silicate divergence in both years. Both results are indicative of a MOC-driven modulation of the biological carbon uptake (by the upper MOC limb) and nutrient inventories (by the lower MOC limb) in the North Atlantic.

1. Introduction

Oceans play a crucial role in the climate system (Siedler et al., 2001). The capacity of the ocean to uptake and store atmospheric CO_2 emitted by human activities buffers the effects of the anthropogenically induced perturbations on the global carbon cycle (Heinze et al., 2015; Khatiwala et al., 2013). This anthropogenic uptake by the solubility pump (2.6 Pg-C yr^{-1}; Gruber et al., 2019) is, however, small compared to the much larger natural carbon cycle including the roughly 10 Pg-C yr^{-1} exported from the upper ocean via the biological carbon pump (BCP) consisting of the production, sinking and remineralization of organic matter (Falkowski et al., 1998; Ito & Follows, 2005). Small changes in natural carbon uptake therefore have the potential to negate or amplify oceanic uptake of anthropogenic carbon. Such changes are likely because the BCP is not homogeneously distributed across the ocean, particularly due to limitations imposed by the lack of nutrients in the photic layer (upper 100–150 dbar) (Carpenter & Capone, 2013; Moore et al., 2013; Pérez et al., 2003). The strongly stratified subtropical gyres are some of the most extensive oligotrophic areas (Emerson et al., 2001), whereas the high latitudes, especially the subpolar North Atlantic (Pommier et al., 2009), are characterized by elevated winter nutrient concentrations which support extensive phytoplankton blooms in spring (Watson et al., 2009).

Nutrients in the upper ocean are provided from multiple sources/mechanisms including coastal runoff, atmospheric deposition, horizontal advection, isopycnal heave, wind-driven upwelling, diapycnal diffusion and/or induction (e.g., Williams & Follows, 2003). The importance of these mechanisms varies by region,

with the Gulf Stream, so called "nutrient stream" (Pelegrí & Csanady, 1991), being key in supplying nutrients from the tropics to the mid and high latitudes in the Atlantic (Williams et al., 2011) and sustaining primary production in the subtropical gyre via lateral advection (Dave et al., 2015; Letscher et al., 2016; Palter et al., 2005, 2011; Pelegrí et al., 2006) and subsequent induction downstream (Williams et al., 2006). The Gulf Stream forms the western boundary of the subtropical gyre and comprises the bulk of the warm northward upper limb of the Atlantic Meridional Overturning Circulation (MOC) (Meinen et al., 2010). Changes in ocean MOC are closely linked with the North Atlantic Oscillation (NAO), the leading mode of atmospheric variability in the North Atlantic, on interannual to decadal timescales (DeVries et al., 2017; Stepanov & Haines, 2014; Sutton et al., 2017). The NAO evolved from largely positive states in the 1990s to near neutral states in the 2000s (Hurrell et al., 2013), reaching exceptionally negative values in 2010 (Osborn, 2011; Stendardo & Gruber, 2012). This extreme negative phase of the NAO in 2010 led to an anomalous southward Ekman transport and a weakening of the MOC at 26.5°N (Srokosz & Bryden, 2015), with potential effects on the nutrient supply to the upper ocean (Cianca et al., 2007; Oschlies, 2001).

Since nutrient availability limits primary production, any change in oceanic nutrient content and supply to the photic layer has the potential to influence the regional magnitude and/or efficiency of the BCP (Stocker et al., 2013). The assessment of basin-scale nutrient pools and their variability is, therefore, crucial to our understanding of how the BCP functions and what factors control its magnitude and efficiency. Several studies have examined the large-scale meridional transport of major nutrients (nitrate, phosphate, and silicate) in the North Atlantic (Álvarez et al., 2002, 2003, 2004; Ganachaud & Wunsch, 2002; Lavín et al., 2003; Martel & Wunsch, 1993; Maze et al., 2012; Rintoul & Wunsch, 1991; Schlitzer, 1988; Williams & Follows, 1998; Williams et al., 2000, 2011), whereas fewer studies have provided nutrient budget estimates in the region (Álvarez et al., 2003; Fontela et al., 2019; Ganachaud & Wunsch, 2002; Maze et al., 2012; Michaels et al., 1996). Due to the differences and limitations of the methodological approaches, whether the North Atlantic is a net source for nutrients to the other basins remains subject to debate (Table 1). The inability to accurately assess time varying sources and sinks, as well as the scarcity of observational data that would allow estimation of accurate tracer accumulation/depletion rates at a basin scale, has traditionally resulted in a steady-state condition becoming a *de facto* assumption for the majority of the inverse nutrient budget calculations. The steady-state assumption implies the nutrient inputs and outputs are in balance so that the basin does not accumulate or lose nutrients in time. Only a very few studies indicated that the North Atlantic nutrient stocks might not be in steady-state on decadal to century time-scales (e.g., Michaels et al., 1996). In this study we re-evaluate the nutrient budgets in the North Atlantic using the wealth of data collected since the last estimates by Álvarez et al. (2003). We consider the response of North Atlantic nutrient budgets to changing circulation and the likelihood that these budgets are not in steady-state on annual-to-interannual timescales, suggesting that the biogeochemical budgets are subject to transient responses to the large (and rapid) MOC changes.

The study is structured as follows: in Section 2, we present the data and methods; in Section 3.1, we examine the basin-scale meridional nutrient (and oxygen) distributions and transports across both sections, accounting for the differences between both occupations (2004 and 2010); next, in Section 3.2, by combining both hydrographic sections and recent estimates of external nutrient sources, we quantify the nutrient budgets of the region between the sections in both years to test the hypothesis that the North Atlantic is in a biogeochemical steady state; and finally, Section 4 contains the summary and conclusions.

2. Data and Methods

2.1. Hydrographic Data

We used the cruise data from the GO-SHIP A05-24.5°N (www.nodc.noaa.gov/ocads/oceans/RepeatSections/clivar_a05.html) and OVIDE (www.nodc.noaa.gov/ocads/oceans/RepeatSections/clivar_ovide.html) sections (Figure 1). Both sections comprise high-quality measurements at high spatial resolution of standard tracers such as temperature, salinity, nitrate, silicate, phosphate, oxygen, and carbonate system variables (pH, alkalinity, and DIC), making them a valuable observational database for the study of the biogeochemical transports in the North Atlantic. First sampled in 1957, the A05-24.5°N section has been occupied nine times over the last few decades. In this study, we used the April–May 2004 (Brown et al., 2010) and January–Feburary 2010 (Atkinson et al., 2012) repeats. Among the nine biennial repeats of the OVIDE section,

Global Biogeochemical Cycles

10.1029/2020GB006898

Table 1
Summary of Reference Observation-Based Estimates of the Meridional Nutrient and Oxygen Transports at Different Latitudes in the North Atlantic

Section	Cruise	Date		Property transport (kmol s^{-1})				Steady-state assumption	Reference
				Silicate	Nitrate	Phosphate	Oxygen		
Davis Strait (67°N)	ARK-XXI 1b	August 16–September 9	2005	−42.9 ± 5.2	−31.3 ± 3.6	−3.7 ± 0.4	np[a]	Yes	Torres-Valdés et al. (2013)
OVIDE (40-60°N)	35TH20020610	June 10–July 12	2002	np	11 ± 16	−0.2 ± 1	−924 ± 314	Yes	Maze et al. (2012)
	35TH20040604	June 4–July 7	2004						
	06MM20060523	May 21–June 28	2006						
	35TH20080610	June 10–July 10	2008	−130 ± 50[a]	10 ± 35[a]	1.1 ± 3.6[a]	−2,070 ± 600[a]	No	Fontela et al. (2019)
	35TH20100610	June 8–July 7	2010						
	29AH20120622	June 23–August 12	2012						
	35PK20140515	May 20–June 26	2014						
	29AH20160617	June 17–July 31	2016						
A25 (40-60°N)	4x	August 7–September 17	1997	−26 ± 15 np	−50 ± 19 −16 ± 36	−6 ± 2 np	−1,992 ± 440 np	Yes	Álvarez et al. (2002) Maze et al. (2012)
A02 (47°N)	29HE06_1-3	July 14–August 15	1993	−130 ± 50	10 ± 35	1.1 ± 3.6	−1,750 ± 500	Yes	Ganachaud and Wunsch (2002)
A03 (36°N)	Leg 1, Atlantis II-109	June 11–July 9	1981	−134 ± 38	119 ± 35	np	−2,940 ± 180	Yes	Rintoul and Wunsch (1991)
A05 (24.5°N)	Leg 3, Atlantis II-109	August 12–September 4	1981	−152 ± 56	−8 ± 39	np	−2,600 ± 120	Yes	Rintoul and Wunsch (1991)
	29HE06_1-3	July 14–August 15	1992	−220 ± 80 −254 ± 176	−50 ± 50 −130 ± 95	−7.6 ± 3.6 −12.6 ± 6.3	−2,070 ± 600 −2,621 ± 705	Yes Argued	Ganachaud and Wunsch (2002) Lavín et al. (2003)
A06 (7.5°N)	35A3CITHER1_2	January 5–February 19	1993	−160 ± 110	−70 ± 120	−1.0 ± 7	−1,430 ± 950	Yes	Ganachaud and Wunsch (2002)

Negative transports meaning southwards.
[a]Average transport estimates also considering the 2002, 2004, and 2006 cruises. np, not provided.

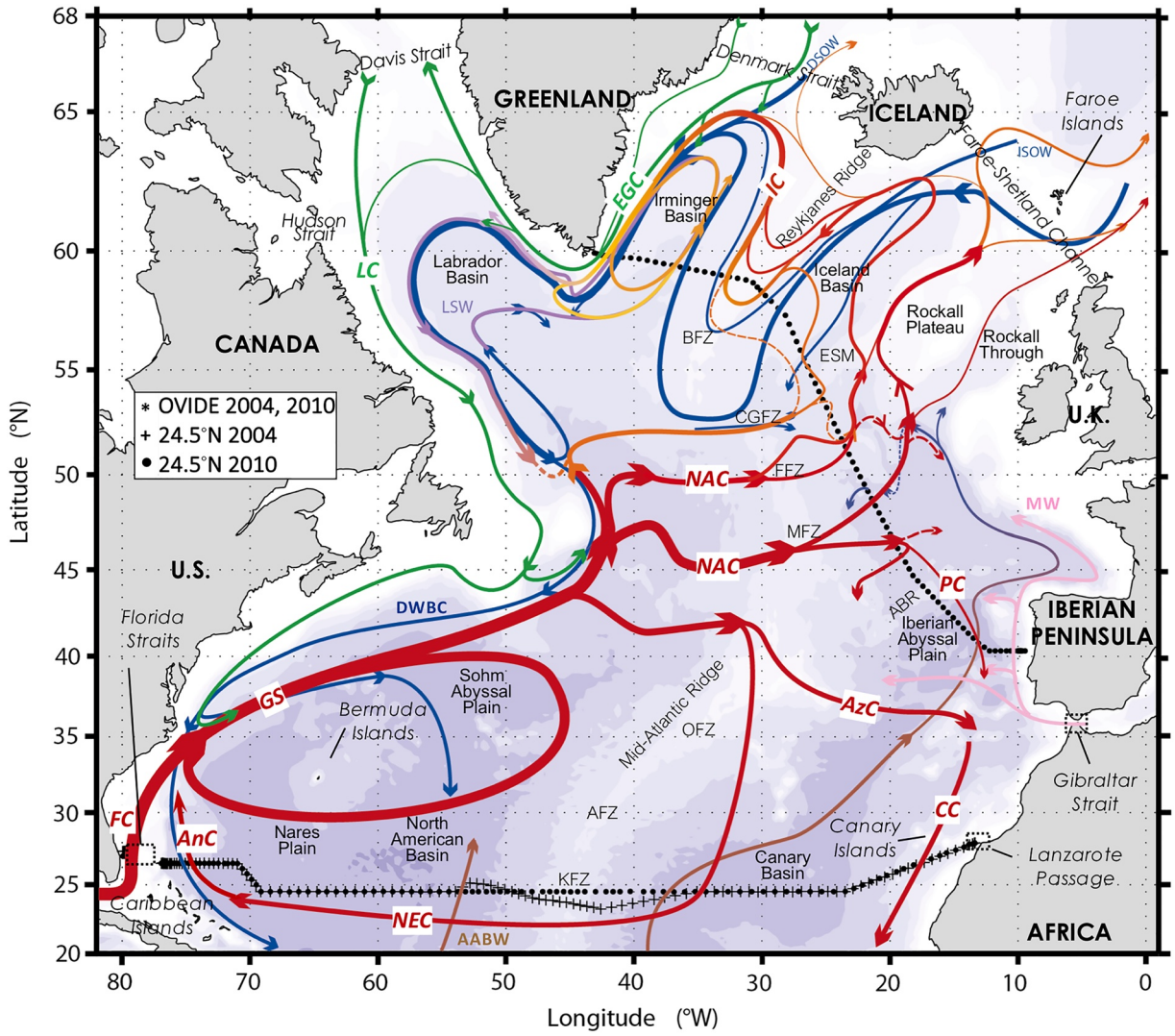

Figure 1. Schematic diagram of the North Atlantic circulation adapted from Daniault et al. (2016). Bathymetry is plotted with color change at 100 m and every 1,000 m at and below 1,000 m. The locations of the A05-24.5°N and OVIDE hydrographic stations are indicated (see legend). The region enclosed by these two sections, and the Davis and Gibraltar Straits, is referred to as NA-box. Major topographic features: Azores-Biscay Rise (ABR), Atlantis Fracture Zone (AFZ), Bight Fracture Zone (BFZ), Charlie–Gibbs Fracture Zone (CGFZ), Eriador Seamount (ESM), Faraday Fracture Zone (FFZ), Kane Fracture Zone (KFZ), Maxwell Fracture Zone (MFZ), and Oceanographer Fracture Zone (OFZ). Labeled water masses and currents: Antarctic Bottom Water (AABW, brown lines), Antilles Current (AnC, red line), Azores Current (AzC, red line), Canary Current (CC, red line), Deep Western Boundary Current (DWBC, blue line), Denmark Strait Overflow Water (DSOW, blue line), East-Greenland Current (ECG, green line), Florida Current (FC, red line), Gulf Stream (GS, red line), Iceland–Scotland Overflow Water (ISOW, blue line), Irminger Current (IC, orange line), Labrador Current (LC, green line), Labrador Sea Water (LSW, purple line), Mediterranean Water (MW, pink line), North Atlantic Current (NAC, red line), North Equatorial Current (NEC, red line), and Portugal Current (PC, red line).

Table 2
List of Hydrographic Cruises Used in This Study

Section	Cruise name	Expocode	Date		Vessel	C.S.	#St	Reference
OVIDE	OVIDE 2004	35TH20040604	June 4–July 7	2004	*Thalassa*	T. Huck	119	Lherminier et al. (2010)
	OVIDE 2010	35TH20100610	June 8–July 7	2010	*Thalassa*	V. Thierry	95	Mercier et al. (2015)
A05-24.5°N	CLIVAR A05 2004	74DI20040404	April 5–May 10	2004	Discovery	S. Cunningham	125	Atkinson et al. (2012)
	A05 2010	74DI20100106	January 6–February 15	2010	Discovery	B. King	135	

C.S. denotes cruise chief scientist, and #St the number of stations.

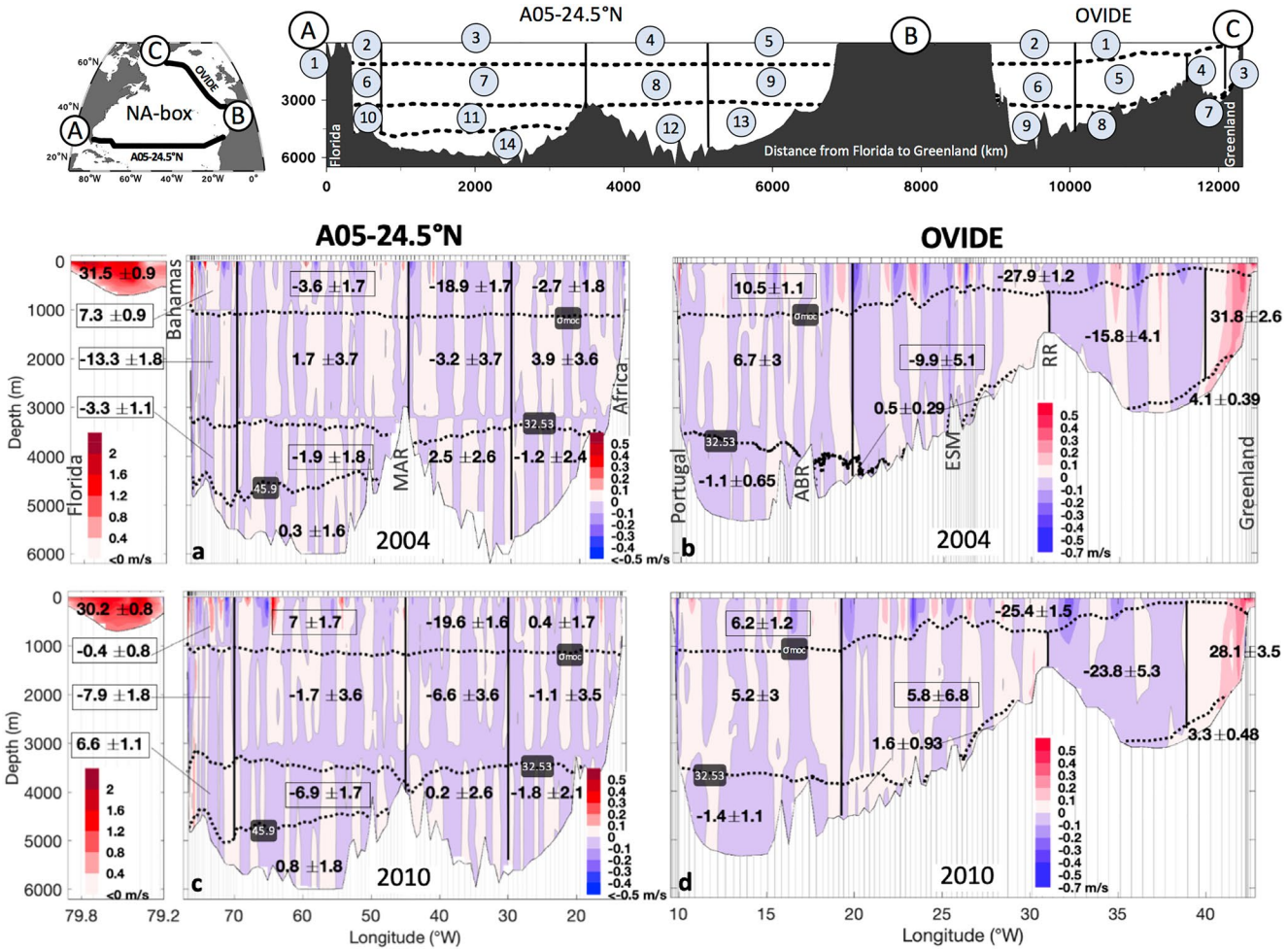

Figure 2. Upper panels: Schematic view of the NA-box (distances are to scale). Numbers in the open circles indicate subregion numeration, as reference for the results section. Lower panels: Velocity (in m/s) perpendicular to the A05-24.5°N (a), (c) and OVIDE (b), (d) sections for the 2004 (upper row) and 2010 (lower row) cruises. Panel b modified from Lherminier et al. (2010). The isopycnals used as density horizons for the nutrient transport estimates are also indicated (dotted lines): σ_{MOC} refers to σ_1 isopycnal 32.15 kg m^{-3} (σ_1 is the potential density referenced to 1,000 dbar), separating the upper and lower limbs of the Atlantic Meridional Overturning Circulation (Mercier et al., 2015); σ_1 = 32.53 kg m^{-3}; σ_4 = 45.9 kg m^{-3} (σ_4 is the potential density referenced to 4,000 dbar). Numbers represent net transports ± uncertainties (in Sv, positive into NA-box) by subregions. Open squares indicate those regions where volume transports are significantly different for both years. Main topographic features are indicated: Azores-Biscay Rise (ABR), Eriador Seamount (ESM), Reykjanes Ridge (RR), Mid-Atlantic Ridge (MAR).

which was first carried out in 2002, we used June–July 2004 (Lherminier et al., 2010) and June 2010 occupations (Mercier et al., 2015) (Table 2). We selected the 2004 and 2010 repeats as they were carried out within the same year at both the subtropical and subpolar locations. Both sections combined together enclose an oceanic region comprising a significant part of the North Atlantic (namely NA-box hereinafter, Figure 2).

In the A05-24.5°N cruises, the analysis of inorganic nutrients, nitrate and nitrite (hereinafter nitrate, NO_3^-), phosphate (PO_4^{3-}) and silicate ($Si(OH)_4$), were undertaken on a Skalar San^{plus} autoanalyzer following the method described by Kirkwood (1996), with the exception that pump rate through the phosphate line was increased by a factor of 1.5 to improve the reproducibility and peak shape of the results. OVIDE nutrients were analyzed using a Chemlab AAII type Auto-Analyzer, following the protocols and methods described by Aminot and Chaussepied (1983). The precision for NO_3^- and $PO_4^{3-}$and $Si(OH)_4$ was evaluated at 0.2, 0.02, and 0.1 μmol kg^{-1}, respectively. Oxygen was determined by Winkler titration, following WOCE standards (Culberson, 1991) and GO-SHIP best practices (Langdon, 2010) at OVIDE and A05-24.5°N, respectively, with a precision better than 1 μmol kg^{-1}. All oxygen and nutrient data were quality controlled (QC)

and corrected according to GLODAPv2.2019 secondary QC protocols (Olsen et al., 2019) (see multiplicative factors in Supporting Information Table S1).

2.2. Other Data Sources

In addition to cruise data, we used complementary hydrographic data (nitrate and neutral density) from the Bermuda Atlantic Time-series Study (BATS) site (http://bats.bios.edu/), as well as MODIS satellite chlorophyll data (https://oceandata.sci.gsfc.nasa.gov/MODIS-Aqua/), Vertical Generalized Production Model (VGPM) Net Primary Production data (Behrenfeld & Falkowski, 1997), and the Hurrell North Atlantic Oscillation (NAO) Index (https://climatedataguide.ucar.edu/climate-data/hurrell-north-atlantic-oscillation-nao-index-station-based) for the period 2004 to 2012, to validate the anomaly signals detected in our data; the RAPID MOC time series data (Smeed et al., 2019), to compute the MOC magnitude for the period of the cruises and the annual averages, as a reference; and different wind product databases: the Cross-Calibrated Multi-Platform Product (CCMP) (Atlas et al., 2011), NCEP (Kistler et al., 2001), and ERA-Interim (Dee et al., 2011), to compute the Ekman transport across the sections.

Finally, to estimate the nutrient budgets in the NA-box (Section 2.4), we also used additional data sources from former studies (Supporting Information Table S2) to account for the external inputs of nutrients by river runoff, atmospheric deposition, N_2-fixation, seafloor weathering, ground water, hydrothermal and meltwater sources, or the nutrient transports across the open boundaries of the domain (Davis and Gibraltar Straits). Further details about derivation of numbers are provided in Supporting Information (Text S1).

2.3. Transports of Nutrients

The transport of a tracer perpendicular to a transoceanic section (T_{tracer}; kmol s^{-1}) is estimated as

$$T_{\text{tracer}} = \sum_{j=\text{stpA}}^{\text{stpB}} \Delta x_j \int_{za}^{zb} \rho_j \left[\text{tracer}\right]_j v_j \, dz, \tag{1}$$

where T_{tracer} is the transport of the tracer (with *tracer* being the general notation for oxygen, O_2; silicate, $Si(OH)_4$; nitrate, NO_3; or phosphate, PO_4^{3-}) spatially integrated and positive (negative) into (out-of) the NA-box. For each station pair j, ρ_j is seawater density profile (kg m^{-3}), $[\text{tracer}]_j = [\text{tracer}](z)$ is the concentration of the tracer (in μmol kg^{-1}), and $v_j = v_j(z)$ is the (absolute) velocity profile (m s^{-1}). Δx is the horizontal coordinate (station pair spacing along the section, in m), with stpA and stpB referring to two different station pairs (note stpA = 1 and stpB = N, with N the total number of stations pairs, when computing the net tracer transport across the entire section). Station pair notation refers to the mid-point between hydrographic stations, so that, for example, stp1 refers to the midpoint between hydrographic stations 1 and 2. z is the vertical coordinate (density, in kg m^{-3}), with za and zb referring to two different depths (note za = surface and zb = bottom, when computing the net tracer transport across the entire section). To match the velocity fields, the oxygen and nutrient distributions were linearly interpolated at the same 1-dbar grid resolution as the velocity fields and averaged across station pairs. For explanatory purposes, the transports of oxygen, nitrate, phosphate and silicate will be referred to hereinafter as kmol-O s^{-1}, kmol-N s^{-1}, kmol-P s^{-1}, and kmol-Si s^{-1}, respectively. Uncertainties for all nutrient transport estimates were estimated based on the uncertainty of each of the component parts of Equation 1 (detailed in Supporting Information Text S2).

Absolute velocities across the A05-24.5°N and OVIDE sections ($v_j(z)$, Figure 2), were obtained by applying a box inverse model method (Mercier, 1986) founded on the least squares formalism. The thermal wind equation is used to compute the relative geostrophic velocity, normal to the hydrographic section, which depends on the *a priori* selected reference layer. The objective of the inversion is to refine the velocity estimates at the reference level by minimizing, in the least squares sense, a set of constraints given by independent estimates (e.g., ADCP measurements and/or integral volume or tracer transports) and the distance to the *a priori* solution. For the A05-24.5°N, OVIDE joint inversion, we selected the reference levels, as well as a number of a priori constraints (Table 3), according to previous studies at the A05-24.5°N section (Lavín et al., 2003; Atkinson et al., 2012) and the OVIDE section (Lherminier et al., 2007, 2010; Mercier et al., 2015), while satisfying salt conservation (Supporting Information Text S3 and Figures S1 and S2).

Table 3
Volume (Sv; 1 Sv = 10^6 m^3 s^{-1}) and Salt (Sv Psu) Transport Constraints Used in the 24.5°N-OVIDE Joint Inverse Model

Constraints	Longitude (°W)	Station pairs	Vertical range	Before inversion *a priori* value	After inversion value	References
OVIDE section						
2004						
Sal conservation	9.5–42.8	121–225	surf-bottom	−41.2 ± 35.0 Sv psu	−41.7	This study[a]
Vol conservation	9.5–42.8	121–225	surf-bottom	−1 ± 3 Sv	−0.9	Lherminier et al. (2010)
Eastern Boundary	9.5–10.7	121–128	surf-σ_2 36.98 kg m^{-3}	−5 ± 3 Sv	−3.1	Lherminier et al. (2010)
Eastern Boundary	9.5–10.7	121–128	σ_2 36.98 kg m^{-3}-bottom	−1 ± 2 Sv	−1.3	Lherminier et al. (2010)
IAP	11.1–16.4	129–145	σ_4 45.85 kg m^{-3}-bottom	−0.8 ± 0.8 Sv	−0.7	Lherminier et al. (2010)
2010						
Sal conservation	9.5–42.8	133–224	surf-bottom	−24.1 ± 35.0 Sv psu	−26.4	This study[a]
Vol conservation	9.5–42.8	133–224	surf-bottom	−1 ± 3 Sv	−0.4	Mercier et al. (2015)
IAP	9.5–22.5	133–174	σ_4 45.84 kg m^{-3}-bottom	−1.0 ± 1.0 Sv	−0.9	Mercier et al. (2015)
A05-24.5°N section						
2004						
Florida Current	77–80	1–8	0–800 dbar	31.8 ± 1.0 Sv	31.5	Baringer and Larsen (2001)
Atlantic Basin	13.4–77	9–120	surf-bottom	−36.4 ± 3.0 Sv	−37.1	Atkinson et al. (2012)
Sal conservation	13.4–80	1–120	surf-bottom	−26.0 ± 35.0 Sv psu	−23.4	McDonagh et al. (2015)
Vol conservation	13.4–80	1–120	surf-bottom	−1 ± 3 Sv	−1.0	This study[a]
2010						
Florida Current	77–80	1–11	0–800 dbar	30.5 ± 0.8 Sv	30.2	Baringer and Larsen (2001)
Atlantic Basin	13.4–77	12–132	surf-bottom	−33.5 ± 3.0 Sv	−34.0	Atkinson et al. (2012)
Sal conservation	13.4–80	1–132	surf-bottom	−26.0 ± 35.0 Sv psu	−21.1	McDonagh et al. (2015)
Vol conservation	13.4–80	1–132	surf-bottom	−1 ± 3 Sv	−0.8	This study[a]

Positive transports mean into the NA-box, that is, southwards across the OVIDE section and northwards across the 24.5°N.
[a]See Supporting Information Text S3 for derivation of numbers.

The ageostrophic Ekman transport was estimated by means of the wind stress fields from the Cross-Calibrated Multi-Platform Product (CCMP) (Atlas et al., 2011), following McCarthy et al. (2012). A comparison between three different wind products, CCMP, NCEP (Kistler et al., 2001) and ERA-Interim (Dee et al., 2011) was done to validate our choice (Supporting Information Figure S3). The Ekman transport was averaged over the year of the cruise (annual average), and added homogeneously in the first 30 m of the water column. For both cruises and locations, seasonal aliasing did not exceed the range of the uncertainties associated with the annual estimates (Supporting Information Text S4). More details about methods and the sensitivity tests performed are provided in the Supporting Information (Texts S5 and S6).

The net volume transports across the study sections were geographically delimited by subregions (Figure 2). We selected the lateral limits of the regions so that they comprised main reference geographic limits and/or main current systems. Horizontally, we defined four main layers by isopycnal levels limiting the main water masses:

i) an upper-intermediate layer embracing the upper limb of the MOC, from surface to σ_1 = 32.15 kg m^{-3} (hereinafter referred to as σ_{MOC}; Mercier et al., 2015), which at 24.5°N is occupied by Central Waters (of North and South Atlantic origin) and Antarctic Intermediate Water (AAIW) (Guallart et al., 2015), and at OVIDE by North Atlantic Central Water (NACW), Subarctic Intermediate Water (SAIW) and Subpolar Mode Water (SPMW) (García-Ibáñez et al., 2015)
ii) an intermediate-deep layer, $\sigma_{MOC} < \sigma_1 \leq$ 32.53 kg m^{-3} ($\sim\sigma_2$ = 36.94 kg m^{-3}), where at 24.5°N there is contribution of Mediterranean Water (MW), Labrador Sea Water (LSW), and upper North Atlantic Deep

Water ($NADW_U$; of which the main source is the lightest vintage of the LSW) (Guallart et al., 2015), and at OVIDE contribution of SPMW, MW, and LSW (García-Ibáñez et al., 2015)

iii) a deep layer, between $\sigma_1 \leq 32.53$ and $\sigma_4 < 45.9$ kg m^{-3}, which main contribution at 24.5°N is the lower North Atlantic Deep Water ($NADW_L$), and at OVIDE lower North East Atlantic Deep Water ($NEADW_L$), Denmark Strait Overflow Water (DSOW), and Iceland–Scotland Overflow Water (ISOW) (García-Ibáñez et al., 2015)

iv) and a bottom layer, $\sigma_4 < 45.9$ kg m^{-3}, only present at 24.5°N, mainly occupied by Antarctic Bottom Water (AABW) (Hernández-Guerra et al., 2014; Guallart et al., 2015)

σ_{MOC} was defined by Mercier et al. (2015) as the density at which the overturning stream function reaches a maximum across the OVIDE section. At these latitudes, using density coordinates provides a more truthful magnitude of the overturning circulation (Lherminier et al., 2010), as it takes into account the fact that most of the East Greenland-Irminger Current (Figure 1) ultimately belongs to the lower limb of the MOC, while the North Atlantic Current (Figure 1) at the same depths belongs to the upper limb (Figures 2b and 2d). At 24.5°N, however, the overturning streamfunction is usually computed in depth coordinates, so that it represents a balance between net northward (southward) flowing water above (below) the depth of maximum overturning, located at around 1,100 m (McCarthy et al., 2015; Smeed et al., 2014). The 1,100 m level at this latitude is though pretty much concordant with the $\sigma_1 = 32.15$ kg m^{-3} isopycnal (Figures 2a and 2c). To be consistent at both locations, we kept the same upper/lower MOC limb interface definition as at the OVIDE section (i.e., $\sigma_{MOC} = \sigma_1 = 32.15$ kg m^{-3}). Transport-weighted properties by the upper and lower MOC limbs were estimated as the total tracer transport across the given MOC limb, divided by the volume transport by that limb.

2.4. Budget Estimates

As the main goal of the study, we estimated the silicate, nitrate and phosphate budgets in the NA-box. The NA-box was defined as the region bounded by the basin-scale subtropical A05-24.5°N section, the subpolar OVIDE section, and the Davis and Gibraltar Straits (Figure 1). The nutrient budgets, which satisfy the salt conservation (Supporting Information, Text S3), were defined as the balance between the following five main terms: lateral nutrient advection across the limits of NA-box (i.e., across the OVIDE section, T_N^{ovide}; the A05-24.5°N section, T_N^{a05}; the Davis Strait, T_N^{davis}; and the Gibraltar Straits, $T_N^{gibraltar}$), the nutrient supply by river runoff (F_N^{runoff}), the input through the air-sea interface within the enclosed domain $\left(F_N^{air-sea}\right)$, the net biological nutrient source/sink term (B), and the time derivative of the nutrient content $\left(\frac{\Delta N}{\Delta t}\right)$:

$$\frac{\Delta N}{\Delta t} = T_N^{ovide} + T_N^{a05} + T_N^{davis} + T_N^{gibraltar} + F_N^{runoff} + F_N^{air-sea} + B \quad (3)$$

where subindex N refers to a general notation for nutrient (either silicate, $Si(OH)_4$; nitrate, NO_3; or phosphate, PO_4^{3-}). T_N^{ovide} and T_N^{a05} are the nutrient transports estimated according to Equation 1 (Section 2.3), whereas T_N^{davis}, $T_N^{gibraltar}$, F_N^{runoff}, and $F_N^{air-sea}$ were obtained and/or inferred from previous studies (Supporting Information, Text S1 and Table S2). The term B accounts for the net balance between the organic matter production (inorganic nutrient sink) and remineralization (inorganic nutrient source), that is, the net storage of organic matter (dissolved and particulate). Note B does not include the biological fixation of N_2, but this is accounted for as an additional term for the nitrate budget equation, that is, an extra addend in Equation 3, corresponding to the balance between biological dinitrogen fixation versus denitrification, $F_{nitrate}^{N2-fixation}$ (Supporting Information, Text S1.5 and Table S2). For silicate, we took into account the additional contribution of submarine groundwater, seafloor weathering, deep-sea hydrothermal sources (Tréguer & De La Rocha, 2013) and sheet-ice melting (Hawkings et al., 2017) as an extra addend in Equation 3, $F_{silicate}^{other}$ (Supporting Information, Text S1.4 and Table S2).

Under a *de facto* steady-state assumption, the North Atlantic basin is not accumulating or losing nutrients ($\Delta N / \Delta t = 0$), so that the balance of inputs minus outputs must equal the biological term B within the box, which consequently becomes the target unknown in Equation 3. More specifically, for the silicate budget,

B accounts for the balance between biogenic silica production by silicifying plankton versus biogenic silica dissolution (silicate regeneration); whereas for nitrate and phosphate, B refers to the balance between photosynthesis versus respiration of organic matter (nitrate/phosphate regeneration). Most production is remineralized (either in surface or at depth), so in an integrated water column sense, B can only represent either: (1) sediment burial (which is a very small term compared to primary production and export production) or (2) accumulation in a small particulate pool or larger dissolved organic pools. In the sense where water column is split (e.g., upper and lower limb, uMOC and lMOC, respectively), B^{uMOC} and B^{lMOC} represent net community production in the upper limb (if $B^{uMOC} > 0$) and remineralization in the lower limb (if $B^{uMOC} < 0$). These indirect estimates B^{uMOC} and B^{lMOC} can be compared, under certain assumptions, with independent estimates of production and remineralization. Significant larger/lower values of B than those obtained by *in situ* measurements may be indicative of the existence of a time tendency in the nutrient budgets (i.e., $\Delta N / \Delta t \neq 0$), as will be discussed in Section 3.2. Furthermore, when it comes to closing the nitrate and phosphate nutrient budgets in the North Atlantic, one agreed limitation among most previous studies in the region (Álvarez et al., 2003; Fontela et al., 2019; Ganachaud & Wunsch, 2002; Michaels et al., 1996) is the contribution of the dissolved organic nutrient source from the subtropics to higher latitudes, suggested as the potential missing counter-balancing flux that might keep the inorganic nutrient pool in the North Atlantic in balance. We, therefore, also assessed the organic nutrient transport at 24.5°N (Supporting Information, Text S1.6).

In this study, we present the nutrient budgets as net budgets (whole-water column integration) and split into upper (surface to σ_{MOC}) and lower (σ_{MOC} to bottom) MOC limb budgets.

3. Results and Discussion

3.1. Nutrient and Oxygen Distribution and Transports Across the A05-24.5°N and OVIDE Sections

3.1.1. Tracer Distribution General Description

The lowest nutrient concentrations are found in surface waters (Figures 3e–3j) where they are consumed by phytoplankton activity, whereas oxygen concentrations in surface waters (Figures 3c and 3d) are relatively high due to direct exchange with the atmosphere (oxygen solubility). At intermediate levels, nutrients increase (oxygen decreases) due to *in situ* remineralization and aging of the water masses (i.e., organic matter remineralization as water masses are laterally advected from their source regions). This biological process is responsible for the highest nitrate and phosphate concentrations at 24.5°N being found at around 700–900 m (maximum remineralization depth) (Figures 3g and 3i), which is also evidenced by the pronounced oxygen minimum (namely oxygen minimum zone, Figure 3c). Deeper in the water column, high oxygen concentrations relate to the recently ventilated LSW (Figures 3c and 3d). Closer to the bottom, high nutrient concentrations (the highest for silicate, Figure 3e) are associated to the AABW, the oldest water mass across the section.

3.1.2. Mean Circulation Patterns

Here, we describe the main circulation patterns at both locations. The transport values shown represent the average of the 2004 and 2010 occupations ± standard error (Table 4).

At 24.5°N, the upper 1,000 dbar (broadly upper MOC limb, $\sigma_1 \leq \sigma_{MOC}$, regions 1 to 5, Figure 3a) are characterized by a net northward transport of oxygen and nutrients as result of the large northward oxygen and nutrient transport by the Florida and Antilles Currents (regions 1 + 2, Figure 3a), which is not compensated by the gyre recirculation (regions 3 + 4 + 5). The lower MOC limb ($\sigma_1 > \sigma_{MOC}$, regions 6 to 14, Figure 3a), comprises a net southward transport of oxygen and nutrients, mainly advected by the Deep Western Boundary Current (DWBC) system (regions 6 + 7 + 10 + 11, Figure 3a). This current represents the largest transport of nutrients and oxygen across the whole section below 1,000 dbar, although there is also a less intense deep southward transport of oxygen and nutrients in the eastern basin (regions 8 + 9 + 12 + 13, Figure 3a). Deeper in the water column, we find the bottom northward transport of oxygen and nutrients related to the AABW (region 14, Figure 3a). Dominated by the lower MOC limb, the net basin-wide (integration across the entire section) transport of oxygen and nutrients across 24.5°N is southwards (Table 4),

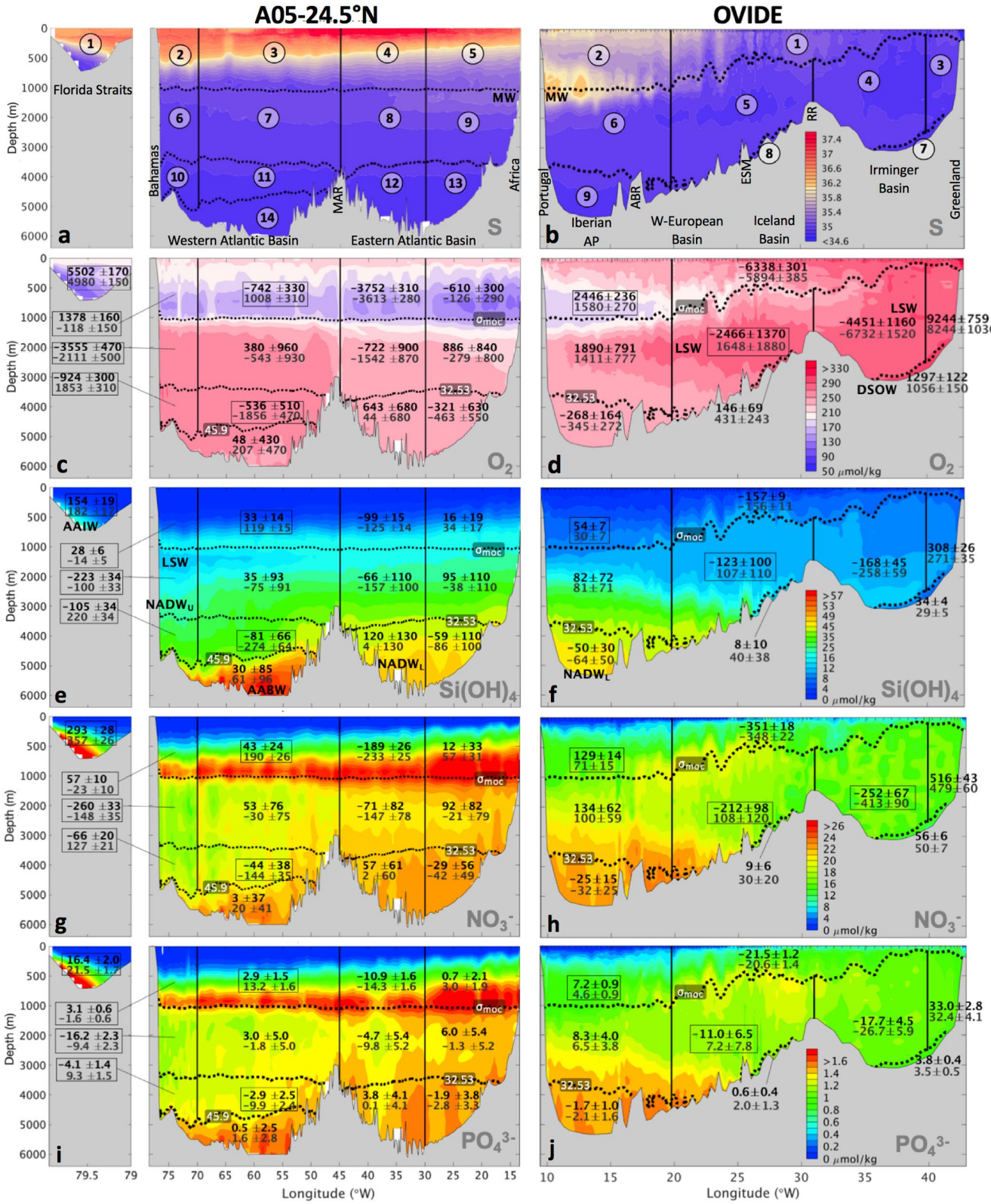
A05-24.5°N
OVIDE
Florida Straits
Bahamas
Africa
MW
MAR
Western Atlantic Basin
Eastern Atlantic Basin
Portugal
ABR
ESM
RR
Iberian AP
W-European Basin
Iceland Basin
Irminger Basin
Greenland
LSW
DSOW
AAIW
NADW$_U$
NADW$_L$
AABW
σ_{moc}
32.53
45.9
S
O_2
$Si(OH)_4$
NO_3^-
PO_4^{3-}
Depth (m)
Longitude (°W)
a
b
c
d
e
f
g
h
i
j

consistent with previous estimates based on the 1992 A05 cruise (July–August) by Lavín et al. (2003) (−2,621 ± 705 kmol-O s^{-1}, −254 ± 176 kmol-Si s^{-1}, −130 ± 95 kmol-N s^{-1}, and −12.6 ± 6.3 kmol-P s^{-1}) and Ganachaud and Wunsch (2002) (−2,070 ± 600 kmol-O s^{-1}, −220 ± 80 kmol-Si s^{-1}, −50 ± 50 kmol-N s^{-1}, and −7.6 ± 3.6 kmol-P s^{-1}).

Across OVIDE, we identify the same upper/lower MOC scheme of circulation, with a net northward transport of oxygen and nutrients by the upper MOC limb ($\sigma_1 \leq \sigma_{MOC}$, regions 1 to 2, Figure 3b), which is mostly carried by the North Atlantic Current (region 1, Figure 3b) and partly recirculates in the easternmost region of the section (region 2, Figure 3b); and a net southward transport of oxygen and nutrients by the lower MOC limb ($\sigma_1 > \sigma_{MOC}$, regions 3 to 9, Figure 3b). At this latitude, different to the A05-24.5°N results, the mean transport of nutrients by the upper and lower MOC limbs is nearly in balance, within the uncertainties; although there is a significant net southward transport of oxygen (Table 4). This result is consistent with estimates reported by Maze et al. (2012) (a three-cruise 2002–2006 mean: 924 ± 314 kmol-O s^{-1}) and Fontela et al. (2019) (an eight-cruise 2002–2016 mean: 909 ± 132 kmol-O s^{-1}). Note, however, the enhanced MOC in 2010 produced nutrient transports that were large enough to be significant (81 ± 49 kmol-Si s^{-1}, 45 ± 19 kmol-N s^{-1}, 6.7 ± 1.3 kmol-P s^{-1}). The only other significant non-zero net nutrient transport across OVIDE in the literature is the Fontela et al. (2019) eight-cruise average phosphate transport (−0.8 ± 0.7 kmol-P s^{-1}). As part of the lower MOC, the Western Boundary Current (East Greenland-Irminger and Deep Western Boundary Currents, region 3, Figure 3b) is the main contributor to the basin-wide transports, comprising an intense southward "deep oxygen and nutrient stream," as observed at 24.5°N. Below, the bottom southward transport related to the DSOW (region 7, Figure 3b) also contributes to the "deep oxygen and nutrients stream". In the European Basin, there is also a deep, albeit less intense, southward flux of oxygen and nutrients between 1,000 and 4,000 dbar pressure range (region 6, Figure 3b). Underneath, in the Iberian Abyssal plain, there is a net northward oxygen and nutrients transport (region 9, Figure 3b).

Between both sections, we estimated an across-σ_{MOC} upward diapycnal flux (1.2 ± 0.7 Sv, 2004 and 2010 average ± standard error of the mean; annual values shown in Figures 5b and 5c) comprising an upward transfer of nutrients between the lower and upper MOC limbs. Although our result is below the uncertainty level, such diapycnal flow is supported by the study of Desbruyères et al. (2013), who found that about 4-Sv, related to the dense-to-light conversion of deep western boundary current waters, fed back into the upper MOC limb in the vicinity of Flemish Cap.

3.1.3. 2004-to-2010 Differences: MOC Limb-Mediated Meridional transports

In this section, we first identify the major differences observed in the oxygen and nutrient distributions and transports in 2010 compared to 2004 at both locations. Temporal variations in oxygen and nutrient distributions may be caused by changes in circulation patterns, that is, more or less of a certain water mass crossing the section, and/or by changes in the tracer concentrations within water masses. Changing water mass tracer concentrations in turn can be the result of changing water mass properties in the source region, changes in the mixing with surrounding waters as the water mass spreads, and/or due to variations in the biological activity. Here, the comparison between both occupations seeks to better understand the representativeness of our estimates with regards to a mean state, as well as the origin of the differences observed, rather than aiming to infer changes over time *per se*.

At 24.5°N, the most striking change was found at the nitrate and phosphate (oxygen) maximum (minimum) depth (Figures 3c, 3g, and 3i), around 700–900 dbar mainly in the Florida Straits and western Atlantic, where the nutrient (oxygen) maximum (minimum) was notably larger (lower) in 2010 compared to 2004 (Fig-

Figure 3. Vertical distribution of salinity (S), oxygen (O_2, in µmol kg^{-1}), silicate ($Si(OH)_4$, in µmol kg^{-1}), nitrate (NO_3^-, in µmol kg^{-1}), and phosphate (PO_4^{3-}, in µmol kg^{-1}) along the A05-24.5°N section (left panels) and the OVIDE section (right panels) for 2004. Numbers in the open circles in panels (a) and (b) indicate sub-region numeration, as reference for the results section. Numbers in panels (c) to (j) represent oxygen and nutrient transports ± uncertainties (in kmol s^{-1}, positive into NA-box) by subregions. Open squares indicate those regions where oxygen and/or nutrient transports are significantly different for both years. The isopycnals used in this study as density horizons for the nutrient transport estimates are also indicated (dotted lines): $\sigma_{MOC} = \sigma_1 = 32.15$ kg m^{-3} (σ_1 is the potential density referred to 1,000 dbar); $\sigma_1 = 32.53$ kg m^{-3}; $\sigma_4 = 45.9$ kg m^{-3} (σ_4 is the potential density referred to 4,000 dbar). Main water masses traceable by the oxygen and nutrient distributions are also indicated: Antarctic Bottom Water (AABW), Antarctic Intermediate Water (AAIW), Denmark Strait Overflow Water (DSOW), Labrador Sea Water (LSW), lower North Atlantic Deep Water ($NADW_L$), Mediterranean Water (MW), upper North Atlantic Deep Water ($NADW_U$); and main topographic features: Azores-Biscay Rise (ABR), Eriador Seamount (ESM), Reykjanes Ridge (RR), Mid-Atlantic Ridge (MAR).

Global Biogeochemical Cycles

10.1029/2020GB006898

Table 4
Mean (2004 and 2010 Average) Volume, Oxygen and Nutrient Transports (±Standard Error of the Mean) by Subregions and by Lower/Upper MOC Limbs

			Tvol (Sv)		Toxy (kmol s^{-1})		Tsil (kmol s^{-1})		Tnit (kmol s^{-1})		Tphos (kmol s^{-1})	
			2004	2010	2004	2010	2004	2010	2004	2010	2004	2010
			Avg		Avg		Avg		Avg		Avg	
OVIDE		Total	−0.9 ± 3.7	−0.4 ± 3.6	1,501 ± 310	1,398 ± 350	−11 ± 28	81 ± 49	4 ± 16	45 ± 19	1.1 ± 1.1	6.7 ± 1.3
			−0.6 ± 0.2		1,450 ± 52		35 ± 46		25 ± 20		3.9 ± 2.8	
		uMOC ($\sigma_1 \leq 32.15$)	−17.3 ± 0.9	−19.2 ± 1.3	−3,892 ± 221	−4,315 ± 324	−103 ± 6	−126 ± 9	−222 ± 12	−277 ± 18	−14.3 ± 0.9	−16 ± 1.1
			−18.3 ± 1		−4,103 ± 211		−115 ± 12		−250 ± 0		−15.2 ± 0.9	
		lMOC ($\sigma_1 > 32.15$)	16.6 ± 1.2	18.8 ± 1.5	5,393 ± 409	5,712 ± 517	92 ± 27	208 ± 49	227 ± 18	322 ± 25	15.4 ± 1.1	22.8 ± 1.7
			17.7 ± 1.1		5,553 ± 160		150 ± 58		274 ± 48		19.1 ± 3.7	
Upper	reg. 1	North Atlantic Current	−26.6 ± 1.3		−6,116 ± 222		−156 ± 0		−350 ± 1		−21 ± 0.4	
	reg. 2	Eastern recirculation	8.4 ± 2.1		2,013 ± 433		42 ± 12		100 ± 29		5.9 ± 1.3	
Intermediate	reg. 3	Western Boundary Current	30 ± 1.8		8,744 ± 500		290 ± 18		498 ± 19		32.7 ± 0.3	
	reg. 4	Irminger Basin	−19.8 ± 4		−5,591 ± 1,141		−213 ± 45		−332 ± 80		32.7 ± 0.3	
	reg. 5	Iceland Basin	−2 ± 7.8		−409 ± 2,057		−8 ± 115		−52 ± 160		−1.9 ± 9.1	
	reg. 6	European Basin	6 ± 0.8		1,651 ± 240		82 ± 0		117 ± 17		7.4 ± 0.9	
Deep	reg. 7	Irminger Basin	3.7 ± 0.4		1,177 ± 433		32 ± 2		53 ± 3		3.6 ± 0.2	
	reg. 8	East Reykjanes Ridge	1 ± 0.5		289 ± 142		24 ± 16		19 ± 10		1.3 ± 0.7	
	reg. 9	European Basin	−1.2 ± 0.1		−307 ± 38		−57 ± 7		−28 ± 3		−1.9 ± 0.2	
A05-24.5°N		Total	−0.98 ± 0.9	−0.8 ± 0.9	−2,326 ± 310	−2,558 ± 310	−122 ± 68	−250 ± 66	−50 ± 40	−33 ± 36	−4.2 ± 2.7	−2.2 ± 2.3
			−0.9 ± 0.1		−2,442 ± 116		−186 ± 64		−42 ± 9		−3.2 ± 1.0	
		uMOC ($\sigma_1 \leq 32.15$)	13.7 ± 0.5	17.5 ± 0.4	1,775 ± 88	2,132 ± 71	132 ± 4	196 ± 4	215 ± 7	349 ± 6	12.3 ± 0.5	21.8 ± 0.4
			15.6 ± 1.9		1,953 ± 178		164 ± 32		282 ± 67		17.1 ± 4.8	
		lMOC ($\sigma_1 > 32.15$)	−14.7 ± 1.7	−18.3 ± 1.4	−4,101 ± 426	−4,690 ± 362	−254 ± 55	−446 ± 48	−265 ± 35	−382 ± 31	−16.5 ± 2.5	−24 ± 2.1
			−16.5 ± 1.8		−4,395 ± 294		−350 ± 96		−323 ± 58		−20.2 ± 3.8	
Upper	regs. 1 + 2 + 3	Florida Straits, W-Atlantic	36.0 ± 0.8		6,004 ± 134		251 ± 36		458 ± 66		27.8 ± 5.3	
	regs. 4 + 5	E-Atlantic	−20.4 ± 1.2		−4,051 ± 312		−87 ± 4		−176 ± 1		−10.7 ± 0.6	
Deep/ Intermediate	regs. 6 + 7 + 10 + 11	DWBC system	−13.3 ± 3.5		−3,646 ± 988		−301 ± 72		−255 ± 62		−16 ± 4.2	
	regs. 8 + 9 + 12 + 13	E-Atlantic	−3.7 ± 5.6		−877 ± 1,362		−94 ± 184		−80 ± 128		−5.3 ± 8.5	
Bottom	reg. 14	W-Atlantic	0.5 ± 0.3		128 ± 79		45 ± 15		12 ± 8		1.1 ± 0.5	

Note. that for the total section and upper and lower MOC limbs, transports by both years are also indicated. Region numbering is illustrated in Figures 2 and 3. Positive (negative) transports mean into (out of) the NA-box.

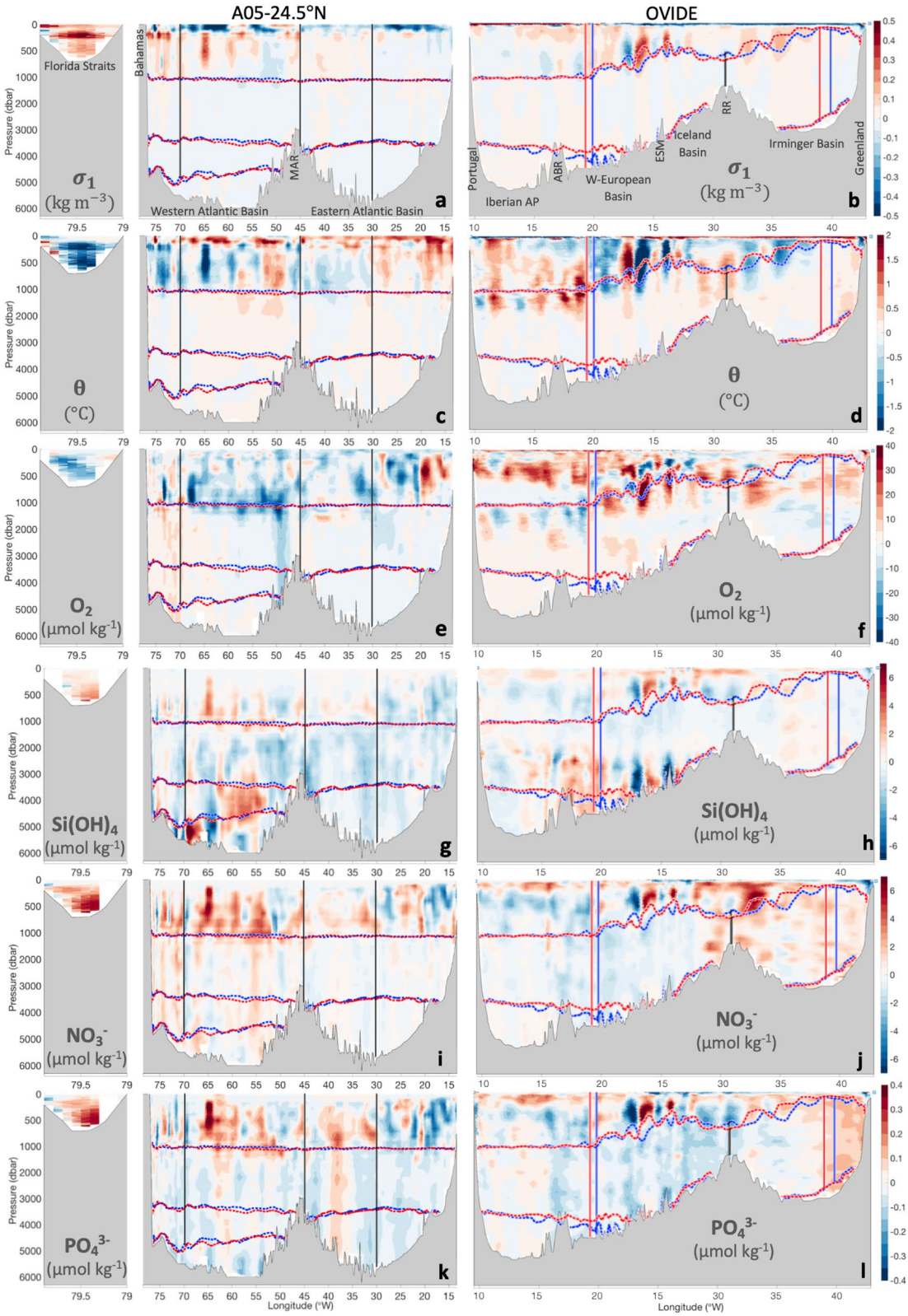

Figure 4. Vertical distributions of potential density (σ_1, potential density referred to 1,000 dbar), potential temperature (θ), oxygen (O_2), silicate ($Si(OH)_4$), nitrate (NO_3^-) and phosphate (PO_4^{3-}) anomalies (2010 minus 2004) on pressure surfaces along the A05-24.5°N section (left panels) and OVIDE section (right panels). The vertical and horizontal colored lines (in blue, 2004; in red, 2010; in black, common to both years) delimit the regions and isopycnal layers used for transport computations in Figure 2.

ures 4e, 4i, and 4k). This large nutrient increase at the thermocline level ranged between 4–7 μmol-N kg^{-1} and 0.2–0.4 μmol-P kg^{-1} in the Florida Straits and Western Atlantic basin, with a section average increase at that level of ∼1 μmol-N kg^{-1} and ∼0.05 μmol-P kg^{-1} (accompanied by a concomitant decrease in oxygen of around 10 μmol kg^{-1}, Figure 4i). Several studies (e.g., Bopp et al., 2002; García et al., 2005, 1998; Matear & Hirst, 2003; Stendardo & Gruber, 2012; Stramma et al., 2010) have reported deoxygenation trends and expansion of hypoxic/suboxic waters at the minimum oxygen zone (broadly 700–1,000 m depth). Yet, the magnitude of these trends (0.6 μmol-O_2 kg^{-1} y^{-1} at 1,100 m for the period 1957–1992 by García et al., 1998; or 0.09–0.34 μmol-O_2 kg^{-1} y^{-1} in the 300–700 m by Stramma et al., 2008) do not account for the 6-year change observed here, evidencing that further driving mechanisms in 2010 might have enhanced the long-term signal. The positive (negative) anomaly signature in nutrients (oxygen) was also accompanied by negative anomalies in temperature (Figure 4c) and salinity (not shown), linked to positive density anomalies (Figure 4a, which can be interpreted as isopycnal vertical displacement (heave).

Evidencing the relevance of these nutrient anomalies, we found that even though the Florida and Antilles Currents were significantly weaker in 2010 (29.8 ± 1.1 Sv; regions 1 + 2, Figure 2c) compared to 2004 (38.8 ± 1.3 Sv; regions 1 + 2, Figure 2a), the nitrate and phosphate transports were not reduced accordingly in proportion (Figures 3g and 3i). That is, the nutrient transport in these regions in 2010 was not dominated by changes in volume transports but compensated instead by changes in nutrient concentration. Overall, both isopycnal heave and the enhancement of the northward transport in the upper western basin in 2010 (regions 2 and 3, Figure 2c) led to more nutrient-rich and less oxygenated thermocline waters being advected to the North (regions 2 and 3, Figures 3e, 3g and 3i). Combined with the gyre recirculation in the eastern basin not being significantly different in both years, this resulted in a significantly larger northward nutrient transport in 2010 by the upper MOC compared to 2004 (Table 4).

In the lower MOC limb, we observed negative silicate anomalies (Figure 4g), especially in the eastern basin. These anomalies were linked to a northward-to-southward flow reversal in 2010 in regions 7 and 9 and enhanced southward flow in region 8 (Figures 2a and 2c), which reduced the influence of southern-origin (silicate-rich) waters in the 1,000-3,500-dbar pressure range compared to 2004. In contrast to this enhanced southward volume transport by the lower MOC in the eastern basin, we found the DWBC system (regions 6 + 7 + 10 + 11, Figure 2) experienced a reduction in 2010 (−9.9 ± 4.5 Sv, Figure 2c) compared to 2004 (−16.8 ± 4.6 Sv, Figure 2a), which was statistically significant in its westernmost branch (regions 6 + 10, Figure 2). This decrease, consistent with the MOC slowdown recorded by the RAPID array (Smeed et al., 2018), led to a concomitant significant reduction of the southward nutrient transports by the DWBC (Figures 3e, 3g, and 3i). West of the Mid-Atlantic Ridge below 3,500 dbar, we also observed positive silicate anomalies (Figure 4g) linked to a larger influence of southern-origin waters in 2010 in this part of the section as result of the reduced DWBC transport (less northern-origin $NADW_L$ influence) (Figures 2a and 2c, regions 10 + 11 + 12). Integrated across the section and from surface to bottom, the anomalous circulation pattern in 2010 resulted in total nitrate and phosphate transports that were not statistically different from zero (Table 4). Compared to the 2004 transports, a reduction of the meridional nitrate and phosphate total transport of 34% and 48%, respectively, was thus observed. Total oxygen and silicate transports were larger in 2010 compared to 2004, although these temporal differences were within the range of the uncertainties.

At OVIDE, the North Atlantic Current (region 1) was weaker in 2010 (Figures 2b and 2d), consistent with the reduction of the Florida and Antilles Currents at 24.5°N. Its southwards recirculation in the eastern basin (region 2) was also reduced in 2010, although this slowdown was more pronounced than the reduction in the North Atlantic Current, leading the net oxygen and nutrient transports by the upper MOC limb to be significantly larger in 2010 compared to 2004 (Table 4). We identified a positive nitrate anomaly (of 5–7 μmol kg^{-1}, Figure 4j) over the Reykjanes Ridge, coincident with an intensification of the Irminger Current (Figures 2b and 2d). The fact that the nitrate anomaly was not accompanied by a concomitant increase in phosphate (Figure 4l), prompted us to hypothesize that the waters advected by the enhanced Irminger Current comprised a larger contribution of subtropical-origin waters, which are characterized by high N_2-fixation-derived nitrate concentrations relative to phosphate, i.e., positive N* (N-16P) anomaly (Benavides et al., 2013; Benavides & Voss, 2015; Gruber & Sarmiento, 1997). These results may comprise observational evidence of how under a negative-NAO scenario, the cyclonic circulation in the Newfoundland Basin strengthens so that the Labrador Current and its retroflection intensify (Henson et al., 2013; Sara-

Table 5
Transport-Weighted Properties (Oxygen, Silicate, Nitrate, Phosphate) by Upper and Lower MOC Limbs (uMOC, lMOC)

		Transport (Sv)		Transport-weighted properties (μmol kg^{-1})							
				Oxygen		Silicate		Nitrate		Phosphate	
		2004	2010	2004	2010	2004	2010	2004	2010	2004	2010
uMOC	OVIDE	−17.3 ± 0.9[a]	−19.2 ± 1.3	218 ± 16[a]	220 ± 22[a]	5.7 ± 0.4[a]	6.4 ± 0.6[a]	12.4 ± 0.9[a,b]	14.1 ± 1.3[a,b]	0.8 ± 0.1	0.8 ± 0.1[a]
	A05	13.7 ± 1.0 [a,b]	17.5 ± 0.9[b]	126 ± 16[a]	119 ± 11[a]	9.4 ± 1.6[a,b]	11.0 ± 1.2[a,b]	15.3 ± 2.6[a,b]	19.4 ± 1.9[a,b]	0.9 ± 0.2[b]	1.2 ± 0.1[a,b]
lMOC	OVIDE	16.6 ± 1.2	18.8 ± 1.5	320 ± 33	295 ± 35[a]	5.5 ± 1.7[a,b]	10.8 ± 2.7[a,b]	13.4 ± 1.4[a,b]	16.6 ± 1.8[a,b]	0.9 ± 0.1[b]	1.2 ± 0.1[b]
	A05	−14.7 ± 1.2[b]	−18.3 ± 1.1[b]	273 ± 34	249 ± 24[a]	16.9 ± 4.8[a,b]	23.7 ± 3.7[a,b]	17.6 ± 2.4[a]	20.3 ± 1.8[a]	1.1 ± 0.2	1.3 ± 0.1

Abbreviation: MOC, meridional overturning circulation.
[a]Superscript indicates a larger-than-uncertainty latitudinal property gradient. [b]Superscript indicates larger-than-uncertainty temporal differences.

fanov et al., 2009). We conjecture that the mixing between the Labrador Current and the NAC waters nearby Flemish Cap (Fratantoni & McCartney, 2010) might have been enhanced in 2010 and caused the observed downstream nitrate anomaly. The unusually large phytoplankton abundances in the central Irminger basin in 2010 were also suggestive of such intensified recirculation (Henson et al., 2013).

In the lower MOC limb, we observed positive nitrate and phosphate anomalies in the Irminger Basin (related to the explanation above), but negative anomalies east of the Reykjanes Ridge up to the Azores-Biscay Rise. These negative anomalies related to a to northward-to-southward flow reversal in the Iceland Basin in 2010 (region 5, Figures 2b and 2d), which led to the advection of more recently ventilated (with lower age) waters across the section in 2010.

The southward intensification of these "secondary" southward deep flows in the eastern basin across both the OVIDE and A05-24.5°N sections counteracted the decrease in the DWBC (Figure 2), hence not resulting in a noticeable annual MOC slowdown, as estimated by the RAPID-array time series (12.8 Sv, April 2009–March 2010 average, McCarthy et al., 2012; Bryden et al., 2014, Smeed et al. 2018; 15.0 [5.1] Sv, January–December 2010 average [standard deviation]; Smeed et al. 2019) but leading instead to a larger MOC in 2010 than in 2004 (Table 4). It is important to remark that the RAPID-array MOC estimates and hydro-cruise MOC estimates are based in completely different methodological approaches. Besides, the hydro-cruise based estimates for 2010 (17.5 ± 0.9 Sv, this study; 16.1 Sv, Atkinson et al., 2012) lie within the standard deviation of the MOC magnitude corresponding to the 2010 annual period, as estimated by the RAPID-Array (15.0 [5.1] Sv, January–December 2010 average [standard deviation], Smeed et al. 2019), hence both estimates remain consistent. But in view of the above, hereinafter, we will refer to a DWBC slowdown in 2010 rather than MOC slowdown.

To better disentangle the overall change in properties between both sections and years, we estimated the transport-weighted concentrations for the upper and lower branches of the MOC (Table 5). Both MOC limbs are characterized by a meridional North-to-South gradient of decreasing (increasing) oxygen (nutrient) concentrations (Figure 3, Table 5). Biotic remineralization of the exported dissolved organic carbon at high latitudes (Fontela et al., 2016), as well as dilution with the northward-flowing low dissolved organic carbon Antarctic Intermediate and Bottom Waters (Hansell et al., 2009), support the observed gradient. Oxygen is furthermore influenced by enhanced solubility of colder subpolar waters (Gruber et al., 2001) and deep convection of recently ventilated waters, which ultimately favors the transfer of this high-oxygen signal to depth (Fröb et al., 2016).

The lower MOC limb is more meridionally homogeneous for oxygen than the upper limb, but with the largest silicate gradient (Table 5). For nitrate and phosphate, the transport-weighted properties suggested a more meridionally homogeneous upper MOC in 2004, but a more meridionally homogeneous lower limb in 2010. Both the upper and lower MOC limbs were enriched in nutrients in 2010 compared to 2004 at both sections. Note, however, that at OVIDE the nutrient increase in the upper limb was only significant for nitrate, whereas at A05-24.5°N the nutrient increase in the lower limb was only significant for silicate. The reduced intensity of the DWBC, which favored the penetration of AABW northwards (Figure 2), would

explain the overall significant increase in the transport-weighted silicate concentration by the lower MOC limb (Table 5).

In summary, in this study we identified an anomalous pattern of advection in 2010 including anomalously negative Ekman transport, isopycnal heave, reorganization in the gyre circulation, and weakening of the DWBC, accompanied by strengthening at depth of the secondary southward advective branches; all of these physical drivers favoring the northward transport of more nutrient-richer waters by the upper MOC limb in 2010 (Table 4, Figure 3), which ultimately led to a reduced southward transport of nitrate and phosphate.

Ultimately, the results above may comprise observational evidence of how under a particularly negative-NAO scenario (Osborn, 2011), and favored by the NAO-induced contraction of the Subpolar Gyre (Chaudhuri et al., 2011; Sarafanov et al., 2009), the contribution of subtropical and southern waters at high latitudes of the North Atlantic is enhanced, and compensating altered circulation patterns at depth observed.

3.2. Nutrient Budgets in the North Atlantic in 2004 and 2010

As an ultimate objective of this study, we provided novel estimates of the major inorganic nutrient inventories (silicate, nitrate and phosphate) in the North Atlantic, which had not been re-evaluated for this region since the former studies of Álvarez et al. (2003) and Ganachaud and Wunsch (2002). For the first time in this region, we combined two basin-scale hydrographic sections (the subtropical A05-24.5°N section and the subpolar OVIDE section) occupied in the same year for two different occupation periods (2004 and 2010), to derive consistent circulations across the sections using a joint inverse model and compute the nutrient transports across them. Combining these basin-wide advective nutrient transports with the most recent estimates of the additional external nutrient sources (e.g., atmospheric inputs and river runoff) (Supporting Information, Table S2), we obtained the net nutrient balance term (term B in Equation 3) for the North Atlantic, which under steady-state (ΔN / Δt = 0) leads to an inferred net biological nutrient source/sink in the NA-box (Figure 5).

3.2.1. Water-Column Integrated Nutrient Budgets

Integrated over the whole water column, the net nutrient balance (term B in Equation 3) was statistically different from zero only in 2010 (B[2010]: −106 ± 83 kmol-Si s^{-1}, 75 ± 42 kmol-N s^{-1}, 7.2 ± 2.7 kmol-P s^{-1}, Figures 5d, 5g, and 5j). In 2004, however, the system was close to balance, with none of the net nutrient balance estimates B being significantly different from zero (B[2004]: −60 ± 75 kmol-Si s^{-1}, 25 ± 45 kmol-N s^{-1}, 0.2 ± 2.9 kmol-P s^{-1}). Results from the sensitivity analysis we performed (Supporting Information, Text S6) showed that these net balance estimates are significantly sensitive to the wind forcing used to solve the velocity field at 24.5°N in 2010 (annual vs. synoptic forcing), with quasi-synoptic wind forcing leading to significantly enhanced nutrient convergence (Supporting Information, Figure S8), hence intensifying the anomalous pattern in 2010. Our annual estimates for 2010 might therefore represent a lower bound of the convergence occurred. However, for nutrient budget estimate purposes, the annual forcing provides a more representative approach of the real state as it prevents aliasing of seasonal imbalances, especially when combining cruises that have been carried out in different seasons (Supporting Information, Text S4); since we would be adding extra uncertainty due to the seasonal imbalance linked to the biological term (balance term B in Equation 3).

For nitrate and phosphate, the net balance term was positive showing that under the steady-state assumption, there is a significant (statistically significant in 2010) net nutrient consumption (75 ± 42 kmol-N s^{-1} and 7.2 ± 2.7 kmol-P s^{-1}), which suggests the region is net autotrophic with biological primary production exceeding respiration (i.e., the basin producing more organic carbon than that being consumed through remineralization). Note that if we also considered the organic nutrient fraction contribution to the inorganic budgets (Supporting Information, Text S1.6, Table S2) the resulting balance term B would be even larger (by 13 ± 6 kmol-N s^{-1}, 3 ± 1 kmol-P s^{-1}, and Text S1.6). Relaxing the steady-state assumption, nevertheless, another plausible explanation could be that the region accumulated nitrate and phosphate during the period ($\frac{\Delta N}{\Delta t} > 0$, in Equation 3). This result contrasts with a former study by Álvarez et al. (2003), whose

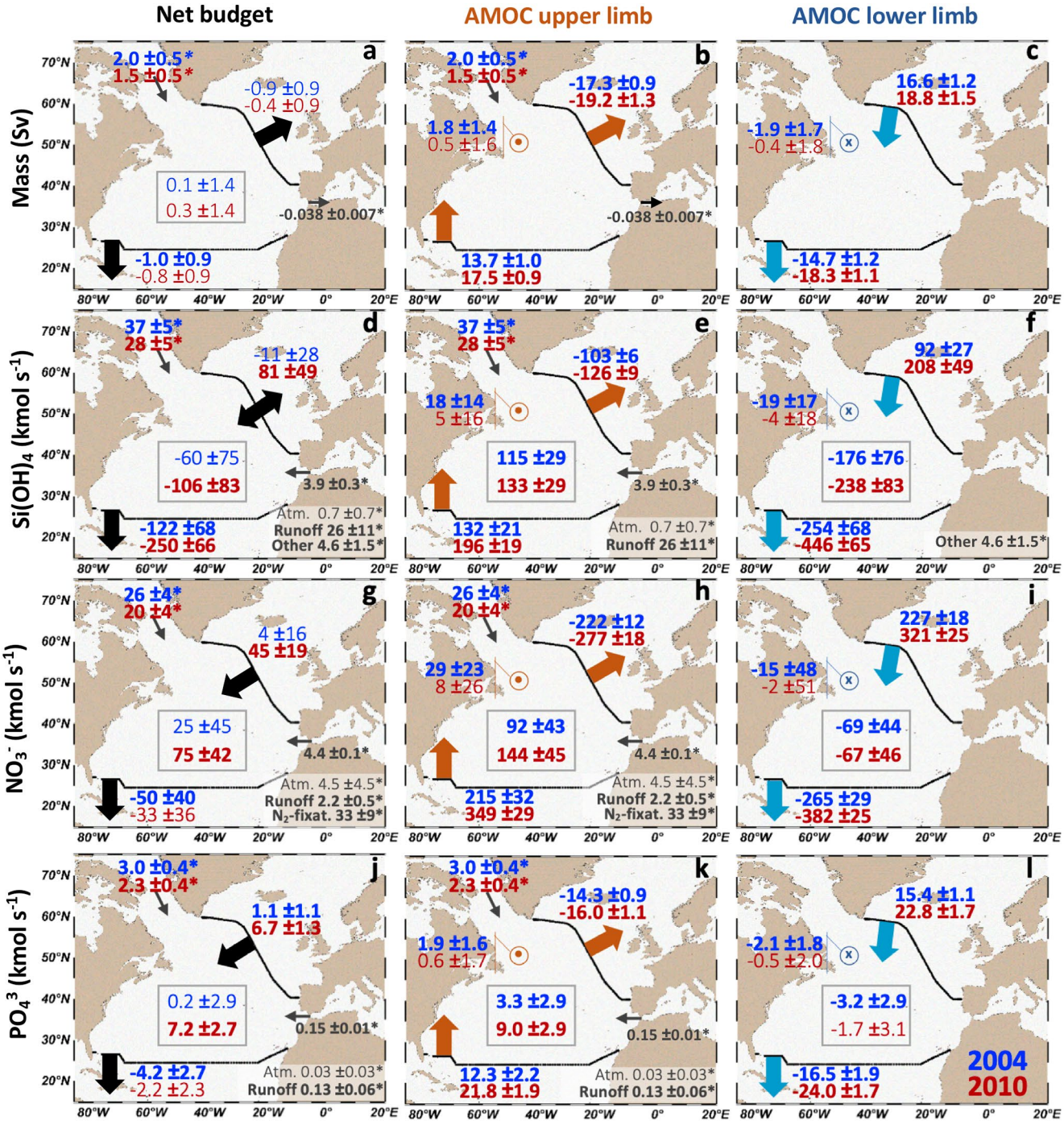

Figure 5. Schematic of the volume ((a) to (c)), silicate ((d) to (f)), nitrate ((g) to (i)) and phosphate ((j) to (l)) budgets in the North Atlantic. Left panels represent the net surface-to-bottom budgets, whereas the middle and left panels account for the upper and lower MOC limb budgets, respectively. Volume budget: numbers in the open square account for the convergence/divergence term closing the budget (positive meaning net evaporation); for the upper (lower) MOC budgets, values outlined in orange point (blue cross) refer to diapycnal flow, positive (negative) sign meaning inflow (outflow). Units in Sv (1 Sv = 10^6 m^3 s^{-1}). Inorganic nutrient budgets: numbers in the open squares account for the net balance term B in Equation 3 (B for the net water-column integrated budget, left side panels; B^{uMOC} for the upper MOC limb budget, central panels; or B^{lMOC} for the lower MOC limb budget, right panels), positive values meaning nutrient convergence (net nutrient consumption under steady-state); negative values meaning nutrient divergence (net nutrient remineralization under steady-state). Units in kmol s^{-1}. Blue (red) numbers refer to 2004 (2010) budgets. Bold font indicates significantly different from zero values. Numbers with an asterisk are referenced in the Supporting Information (Table S2). MOC, meridional overturning circulation.

estimates pointed to a total nitrate production in the North Atlantic region. Their estimate, the result of the sum of a net nitrate consumption between their 4x (OVIDE-like) section and 36°N, and a net nitrate remineralization between 36° and 24.5°N, was however not significantly different from zero (15 ± 131 kmol s^{-1}), which makes it statistically comparable to our result in 2004.

Contrarily to nitrate and phosphate, the water-column integrated silicate budget resulted in a negative balance term. For both years, the net silicate balance (B[2004]: −60 ± 75 kmol-Si s^{-1}; B[2010]: −106 ± 83 kmol-Si s^{-1}; its magnitude being only statistically significant in 2010) indicated net silicate regeneration within the NA-box (i.e., net loss of biogenic silica, under the steady-state assumption). Or, relaxing the steady-state assumption, it might be indicative of the North Atlantic losing silicate during the period ($\frac{\Delta N}{\Delta t} < 0$, in Equation 3).

The opposing sign in the water-column integrated net silicate balance versus that of nitrate and phosphate, indicated a different pattern for these nutrients. The NA-box is a region that comprises part of the subtropical and subpolar gyres, and where a number of different biogeochemical provinces coexist (Reygondeau et al., 2013). Hence, changes in relative abundances of the non-siliceous phytoplankton (requiring nitrate and phosphate but not silicate) and diatom phytoplankton communities (which in addition to phosphate and nitrate require silicate) might partly explain the differential response observed in the silicate versus nitrate and phosphate budgets.

3.2.2. Nutrient Budgets by the Upper and Lower MOC Limbs

We now split the inventories into upper/lower MOC limbs to better understand the observed imbalances and their interpretation, as well as to further understand the differences between the 2004 and 2010 total nutrient budgets.

3.2.2.1. Upper-MOC Nutrient Budgets

The upper limb of the MOC within the NA-box domain was unequivocally characterized by a net positive balance of inorganic nutrients ($B^{uMOC} > 0$; Figures 5e, 5h, and 5k). Under steady-state conditions, this excess of nutrients should be entirely accounted for by the biological term, that is, the upper limb being characterized by net nutrient consumption (organic matter production exceeding remineralization). Our results also show that nutrient consumption was enhanced in 2010 (B^{uMOC}[2010]: 133 ± 29 kmol-Si s^{-1}, 144 ± 45 kmol-N s^{-1}, 9.0 ± 2.9 kmol-P s^{-1}, Figures 5e, 5h, and 5k, red numbers) compared to 2004 (B^{uMOC}[2004]: 115 ± 29 kmol-Si s^{-1}, 92 ± 43 kmol-N s^{-1}, 3.3 ± 2.9 kmol-P s^{-1}; Figures 5e, 5h, and 5k, blue numbers), although this enhancement was only statistically significant for the phosphate budget (5.7 ± 4.1 kmol-P s^{-1}). To put numbers into context with the biological carbon pump, this enhancement in the uMOC phosphate consumption, translated into carbon via stoichiometric ratios of C:N:P:O_2 = 117:16:1:−170 (Anderson & Sarmiento, 1994), is equivalent to an increase in organic matter production of 0.25 ± 0.18 Pg-C yr^{-1} in 2010 (1.7 times the value in 2004, 0.14 Pg-C yr^{-1}). For comparison, the mean annual sea-air CO_2 flux in the North Atlantic (north of 14°N, including the Nordic Seas and portion of the Arctic) is −0.49 Pg-C yr^{-1} (Takahashi et al., 2009) of which our estimate of the anomalous 2010 uMOC nutrient budget represents up to 50%. Note, however, our indirect estimate should be taken as an upper-bound value, as we are assuming steady-state (no nutrient accumulation). Note as well the upper MOC limb is deep enough for remineralization to take place too, so our estimate represents the net balance between consumption of "new" nutrients in the euphotic zone (transferred to depth via the BCP) and their remineralization deeper in the water column within the upper limb.

The high-nutrient signature observed at 24.5°N in 2010 was also identifiable downstream in the North Atlantic by an independent data source at BATS station (Figure 6e). The combination of a larger nutrient supply by horizontal advection with the heave of the isopycnals in the western-inner gyre (Figure 6d), and subsequent upwelling of those nutrients to the sunlit upper ocean (Figure 6e), altogether favored an (immediate) biological response (enhanced primary production/nutrient consumption) in the upper ocean between 26.5° and 40°N (Figures 6b and 6c) and likely in the subpolar gyre (Henson et al., 2013). Actually, our results indicate that the missing nutrient source reported by Henson et al. (2013) may actually have had a subtropical origin.

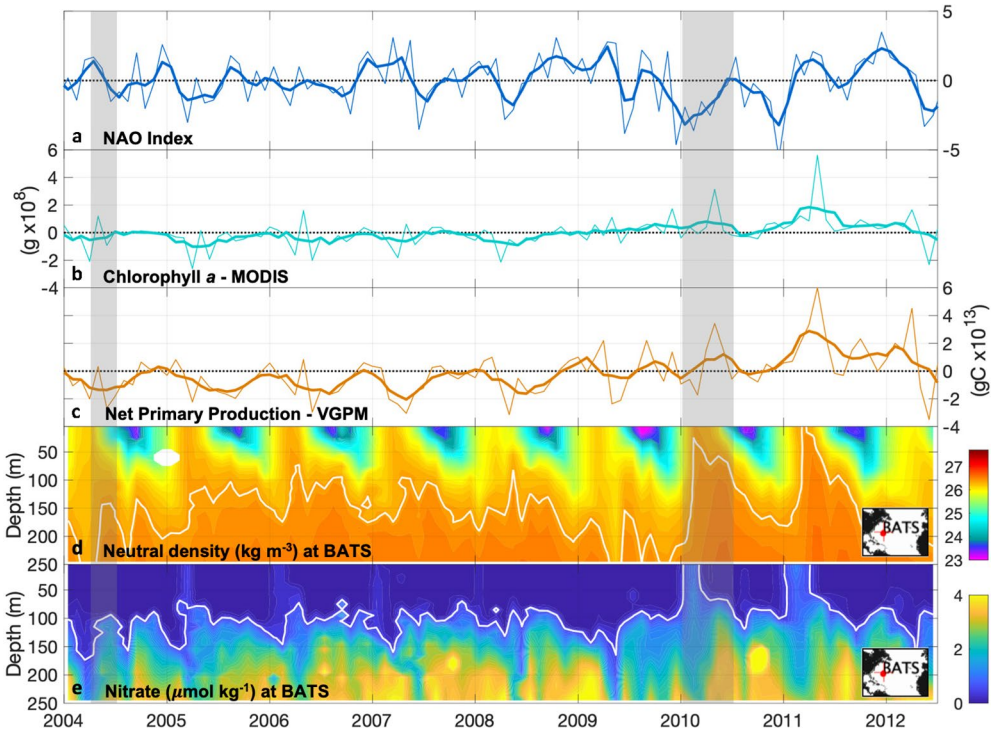

Figure 6. Time-series of (a) Hurrell North Atlantic Oscillation (NAO) Index, (b) MODIS satellite Chlorophyll *a* anomalies (deseasonalized, mean removed) for 20°–50°N, 5°–80°W, (c) Vertical Generalized Production Model (VGPM) Net Primary Production anomalies (deseasonalized, mean removed) for 20–50°N, 5–80°W, (d) neutral density, and (e) nitrate 2004–2013 time series at the Bermuda Atlantic Time-Series (BATS) station. Bold lines in panels (a) to (d) equate to 3-month filter applied. The white line in panel (d) indicates the $\gamma_n = 26.35$ kg m^{-3} isopycnal and the white line in panel (e) indicates the isoline of 0.5 μmol kg^{-1} nitrate concentration. BATS, Bermuda Atlantic Time-Series; NAO, North Atlantic Oscillation. Grey shading indicates the timespan covered by the 2004 and 2010 cruises.

In summary, this study provides evidence that biological CO_2 uptake was boosted in 2010, under anomalously negative NAO conditions (Figure 6a). And not only that, but the time series in Figure 6 also show that the 2010 event was associated with the first large positive anomaly in primary production for the period between 2004 and 2012, which was followed by an even larger positive anomaly in chlorophyll *a* (Figure 6b) and net primary production (Figure 6c) next spring. This second anomaly is hypothesized here to have followed a similar physical mechanism as for the re-emergence of the temperature anomalies reported by Taws et al. (2011). This re-emergence is the process by which the anomalies established over the deep winter mixed layer in winter 2009/2010 were sequestered beneath the seasonal thermocline in summer and reappeared at the surface as the mixed layer deepened during the following winter season (2010/2011), as seen for density and nitrate re-emerging signatures at the BATS site in early 2011 (Figures 6d and 6e).

In adddition, and according to our results, the 2010 anomalous circulation pattern not only led to an enhanced nutrient convergence by the overturning upper limb, but also led to heat convergence within the NA-box to be reduced by 38% in 2010 compared to 2004 (not shown). Our estimate accounts for up to 40% contribution to the total heat content decrease of -1.2×10^{22} J reported by Cunningham et al. (2013), suggesting that not only the biological carbon pump within the NA-box region was favored in 2010, but also the heat convergence decrease could have favored a solubility-driven carbon uptake.

3.2.2.2. Lower-MOC Nutrient Budgets

Conversely, the lower MOC limb was characterized by a net nutrient divergence, its magnitude exceeding the uncertainty level for silicate.

Nitrate and Phosphate

For the nitrate and phosphate lower MOC budgets, we obtained net balance terms (B^{lMOC}[2004]: -69 ± 44 kmol-N s^{-1}, -3.2 ± 2.9 kmol-P s^{-1}; B^{lMOC}[2010]: -67 ± 46 kmol-N s^{-1}, -1.7 ± 3.1 kmol-P s^{-1}) consistent with organic carbon consumption at depth of about 0.19 ± 0.13 Pg-C yr^{-1} (based on the 2004 and 2010 average nitrate estimates) or 0.11 ± 0.13 Pg-C yr^{-1} (based on the 2004 and 2010 average phosphate estimates). Our estimates, although largely uncertain, can be compared with the net DOC consumption rate estimated by Fontela et al. (2016) for the lower MOC limb (0.062 Pg-C yr^{-1}) which would be combined with remineralization of sinking POC.

Silicate

For the silicate budget, we found the largest divergence of the three nutrients (176 ± 76 kmol-Si s^{-1} in 2004; significantly larger in 2010, 238 ± 83 kmol-Si s^{-1}). Under the steady-state assumption (no net nutrient accumulation/loss), such divergence indicates net remineralization within the lower MOC limb, as might be expected. In an *in situ* study in the deep northeast Atlantic (3,000-m depth), Ragueneau et al. (2001) estimated an annual opal flux of 43.0 mmol-Si m^{-2} yr^{-1} (i.e., 23 kmol-Si s^{-1}), subject to a seasonal fluctuation between ~6 kmol-Si s^{-1} in autumn/winter and ~133 kmol-Si s^{-1} in spring/summer (Ragueneau et al., 2001). When averaged with other *in situ* estimates at different sites in the North Atlantic, the mean opal flux decreases to about 16 kmol-Si s^{-1} (0.03 mol m^{-2}, Ragueneau et al., 2000). Since most of biogenic silica production is exported to deeper levels more efficiently than particulate organic carbon (Segschneider & Bendtsen, 2013) and mostly recycled within the water column (Loucaides et al., 2012; Tréguer et al., 1995), we could take these *in situ* measurements of opal flux as a reference. Any of the *in-situ* estimates, however, are significantly lower than our inferred rate. Hence, we hypothesize that the silicate divergence might actually not be completely balanced by the biological remineralization term, but instead there might be also a net silicate divergence in the lower MOC limb (silicate pool decreasing in time). However, given the large uncertainties and current limitations on the nutrient budget assessment, as well as the debateable comparability between basin-scale budget and sediment-trap derived estimates, this interpretation is not conclusively supported by this study but only hypothesized.

3.2.3. Further Considerations on the Nutrient Budget Estimates

In this study, we revisited the external nutrient sources (e.g., river runoff and atmospheric input) based on the most recent studies. As illustration, the atmospheric and river runoff nitrate supply used in this study (4.5 ± 4.5 and 2.2 ± 0.5 kmol-N s^{-1}, respectively) were larger than those formerly used in the study by Álvarez et al. (2003) (3.7 and 1.4 kmol-N s^{-1}, respectively). The ongoing anthropogenic forcing is very likely to keep increasing the nutrient supply via atmospheric and river runoff, as evidenced by the trend over the last few hundred years (Beusen et al., 2016; Moore et al., 2013; Seitzinger et al., 2010), making them a crucial gateway by which land-based human perturbations are transferred to the open ocean (Duce et al., 2008; Jickells et al., 2017). However, the paucity of observations and the poor understanding of its variability mean estimates of external nutrient sources remain uncertain.

Despite this uncertainty, one important remark is that summed up together, the external nutrient sources comprise a minor term compared to the magnitude of lateral advection. Hence, it is not surprising that changes in ocean circulation patterns might drive major oceanic nutrient pool reorganization on interannual time-scales (this study), or longer (e.g., decadal-centennial) timescales (Riebesell et al., 2009; Schmittner, 2005). Climate change projections predict that the MOC will decrease during the following century (IPCC, 2019), accompanied by a general warming of the sea surface and subsequent ocean stratification (Stocker et al., 2013) and, ultimately, by a reduction in primary productivity (Behrenfeld et al., 2006). However, the mechanistic understanding of the regional drivers at seasonal to multidecadal timescales, as well as the temporal and spatial coherences, is still work in progress. Promising results are now being published on global ocean biogeochemistry models that assimilate both physical and biogeochemical observations (e.g., ECCO-Darwin; Carroll et al., 2020), adding improvement to previous non-assimilation-based models (e.g., Aumont et al., 2015; Galbraith et al., 2010; Stock et al., 2014; Yool et al., 2013). Ocean biogeochemical models have the ability to resolve the spatiotemporal scales necessary for attributing fluxes to their respec-

tive mechanisms, which along with the new capability of the emerging data-assimilative models to optimize the model's fit to observations in a property-conserving manner (Carroll et al., 2020), result in a quantitative description of the time-varying global ocean biogeochemical state, making them a potentially ideal tool for ocean carbon budget studies. However, since these novel state-estimates are still in the evaluation phase, observation-based results remain a valuable and crucial reference for ocean carbon and nutrient budget estimates, despite the large uncertainties inherent to synopticity and sampling biases. Even more if we take into account that rapidly growing autonomous biogeochemical measurement platforms (e.g., Bittig et al., 2019) are augmenting considerably the data spatial and temporal coverage, which ultimately will contribute to reduce sampling bias. Hence, observation-based estimates can, and should, continue to be used as a comparison during model evaluation.

In this study, we have shown that the DWBC slowdown event in 2009/2010, which was accompanied by horizontally driven upper nutrient redistribution, actually conveyed an increase in nutrient convergence in the upper MOC limb and nutrient supply to the upper ocean, which ultimately favored primary production and biological carbon uptake. Therefore, under the ongoing (and projected) scenario of MOC slowdown and increasing ocean stratification, extreme events injecting nutrients to the upper ocean may gain relevance in boosting biological carbon uptake in the North Atlantic.

4. Summary and Conclusions

This study provided new observational basin-scale meridional nutrient transport estimates across the A05-24.5°N and OVIDE sections for the 2004 and 2010 cruises. Both sections are characterized by an upper northward (low-oxygen and low-nutrient) MOC branch carrying nutrients and oxygen to the North Atlantic, and a lower (well oxygenated and nutrient-rich) branch advecting oxygen and nutrients back to the South Atlantic. As result, this overturning pattern drives a net north-to-south meridional transport of nutrients and oxygen, so that the North Atlantic ventilates the South Atlantic and provides it with nutrients.

Lateral advection, and this upper/lower limb overturning circulation pattern, was shown as a key mechanism involved in the meridional flux of nutrients, with the Gulf Stream and its extension downstream, the North Atlantic Current, corroborated as the main advective path for the northward transfer of nutrients from low to high latitudes in the upper MOC limb; and the Deep Western Boundary Current identified as the main "*deep nutrient stream*" by the lower limb, redistributing these nutrients southwards. Although volume transport variations dominated the observed changes in the nutrient transports in most of the regions, we showed that the nutrient transport by the Gulf Stream, particularly at subtropical latitudes, was also greatly influenced by changes in nutrient concentrations, which counteracted opposing changes in volume transport in 2010.

We highlighted in this study the relevance of assessing the varying role the upper and lower MOC limbs play in the transport of oxygen and nutrients, and more importantly the imbalance between both limbs, to better understand the magnitude and variability of the total water-column nutrient inventories.

First assuming steady-state, we estimated the inorganic nutrient budgets in the North Atlantic. Under this assumption, the convergence of nutrients in the upper MOC limb is balanced by net biological consumption, likewise net divergence of nutrients in the lower MOC limb is balanced by net biological regeneration, both consistent with a downward particle flux by the BCP within the region. However, our results showed *higher-than-in-situ* (silicate) remineralization rates in the lower MOC limb, so we suggest that the steady-state assumption may be compromised over the observational period. Even if external nutrient sources (e.g., atmospheric input, river runoff) may become a more relevant input as anthropogenic forcing continues (e.g., by ice sheet melting, or increasing atmospheric dust supply), they still comprise a smaller magnitude term compared to lateral advection (particularly for silicate), so that changing circulation patterns are likely to dominate nutrient budget variability.

As illustration, in 2010, we found a significant enhanced northward transport of more nutrient-rich waters by the upper MOC limb linked to a heave of isopycnals, which favored an (immediate) biological response (enhanced nutrient -nitrate and phosphate-consumption) in the upper ocean between 26.5°–40°N. As result, the water-column integrated nitrate and phosphate budgets in 2010 showed significant net biological

production, pointing to the region as being autotrophic, and demonstrating that extreme events in the atmospheric forcing, and subsequent ocean dynamics reorganization, are capable of driving (boosting) biological CO_2 uptake.

In summary, we showed that the *de facto* steady-state assumption may not be the best representation of the biogeochemical budgets, which may actually be responding on interannual time scales to circulation changes with either accumulation/depletion of the nutrient inventories in response to an excess of nutrient convergence/divergence. However, the large uncertainties associated with the nutrient sources, transports and budgets preclude an irrefutable conclusion. Therefore, we strongly encourage further research to be directed in better resolving the feedbacks between the changes in global circulation patterns and their impact on carbon and nutrient inventories in the ocean, as well as to better quantify the magnitude and variability of the external nutrient sources.

Data Availability Statement

The authors also thank the programs that made cruise data available: GO-SHIP (www.go-ship.org), CLIVAR (www.clivar.org) and CCHDO (cchdo.ucsd.edu). Florida Current absolute transports are also available online (www.aoml.noaa.gov/phod/floridacurrent), as well as Florida Straits repeated hydrography (ftp://ftp.aoml.noaa.gov/phod/pub/WBTS/WaltonSmith/). The computer codes used to analyze the data are available from the corresponding author on reasonable request.

Acknowledgments
This study is a contribution to OVIDE (co-funded by the IFREMER, CNRS/INSU/LEFE), Blue-Action (EU Horizon 2020 grant agreement No 727852), ABC-Fluxes (NERC-funded grant No NE/M005046/1) projects, and CLASS (NERC National Capability Science Single Centre awards) programme. This study was supported by the TRIATLAS project (EU Horizon 2020 grant agreement No 817578). L. I. Carracedo supported by the University of Vigo through the Galician I2C Plan for postdoctoral research, NERC within the framework of the ABC-Fluxes Project, and IFREMER. H. Mercier was financed by CNRS; E. McDonagh and R. Sanders by NERC and NORCE; G. Rosón by the University of Vigo; C. M. Moore and P. Brown by NERC; S.Torres-Valdés by AWI; P. Lherminier by IFREMER; and F. F. Pérez by the BOCATS2 project (PID2019-104279GB-C21) co-funded by the Spanish Government and the FEDER, and by the COMFORT project (EU Horizon 2020 grant agreement No 820989). The authors are grateful to the captains, crew, technicians, and scientists who contributed to the acquisition, processing, and quality control of the hydrographic data used in this study. The authors particularly thank P. Zunino for her valuable contribution to the OVIDE data interpolation.

References

Álvarez, M., Bryden, H. L., Pérez, F. F., Ríos, A. F., & Rosón, G. (2002). Physical and biogeochemical fluxes and net budgets in the subpolar and temperate North Atlantic. *Journal of Marine Research*, *60*, 191–226. https://doi.org/10.1357/00222400260497462

Álvarez, M., Pérez, F. F., Bryden, H., & Ríos, A. F. (2004). Physical and biogeochemical transports structure in the North Atlantic subpolar gyre. *Journal of Geophysical Research*, *109*(C3). https://doi.org/10.1029/2003JC002015

Álvarez, M., Ríos, A. F., Pérez, F. F., Bryden, H., & Rosón, G. (2003). Transports and budgets of total inorganic carbon in the subpolar and temperate North Atlantic. *Global Biogeochemical Cycles*, *171002*(1). https://doi.org/10.1029/2002GB001881

Aminot, A., & Chaussepied, M. (1983). *Manuel des analyses chimiques en Milieu Marin*. Publications du CNEXO, 395 p.

Anderson, L. A., & Sarmiento, J. L. (1994). Redfield ratios of remineralization determined by nutrient data analysis. *Global Biogeochemical Cycles*, *8*(1), 65–80. https://doi.org/10.1029/93GB03318

Atkinson, C. P., Bryden, H. L., Cunningham, S. A., & King, B. A. (2012). Atlantic transport variability at 25°N in six hydrographic sections. *Ocean Science*, *8*(4), 497–523. https://doi.org/10.5194/os-8-497-2012

Atlas, R., Hoffman, R. N., Ardizzone, J., Leidner, S. M., Jusem, J. C., Smith, D. K., & Gombos, D. (2011). A cross-calibrated, multiplatform ocean surface wind velocity product for meteorological and oceanographic applications. *Bulletin of the American Meteorological Society*, *92*(2), 157–174. https://doi.org/10.1175/2010BAMS2946.1

Aumont, O., Ethé, C., Tagliabue, A., Bopp, L., & Gehlen, M. (2015). PISCES-v2: An ocean biogeochemical model for carbon and ecosystem studies. *Geoscientific Model Development*, *8*(8), 2465–2513. https://doi.org/10.5194/gmd-8-2465-2015

Baringer, M. O. N., & Larsen, J. C. (2001). Sixteen years of Florida Current Transport at 27° N. *Geophysical Research Letters*, *28*(16), 3179–3182. https://doi.org/10.1029/2001GL013246

Behrenfeld, M. J., & Falkowski, P. G. (1997). A consumer's guide to phytoplankton primary productivity models. *Limnology & Oceanography*, *42*(7), 1479–1491. https://doi.org/10.4319/lo.1997.42.7.1479

Behrenfeld, M. J., O'Malley, R. T., Siegel, D. A., McClain, C. R., Sarmiento, J. L., Feldman, G. C., et al. (2006). Climate-driven trends in contemporary ocean productivity. *Nature*, *444*(7120), 752–755. https://doi.org/10.1038/nature05317

Benavides, M., Bronk, D. A., Agawin, N. S. R., Pérez-Hernández, M. D., Hernández-Guerra, A., & Arístegui, J. (2013). Longitudinal variability of size-fractionated N2fixation and DON release rates along 24.5°N in the subtropical North Atlantic. *Journal of Geophysical Research: Oceans*, *118*(7), 3406–3415. https://doi.org/10.1002/jgrc.20253

Benavides, M., & Voss, M. (2015). Five decades of N_2 fixation research in the North Atlantic Ocean. *Frontiers in Marine Science*, *2*(40). https://doi.org/10.3389/fmars.2015.00040

Beusen, A. H. W., Bouwman, A. F., Van Beek, L. P. H., Mogollón, J. M., & Middelburg, J. J. (2016). Global riverine N and P transport to ocean increased during the 20th century despite increased retention along the aquatic continuum. *Biogeosciences*, *13*(8), 2441–2451. https://doi.org/10.5194/bg-13-2441-2016

Bittig, H. C., Maurer, T. L., Plant, J. N., Schmechtig, C., Wong, A. P. S., Claustre, H., et al. (2019). A BGC-argo guide: Planning, deployment, data handling and usage. *Frontiers in Marine Science*, *6*(1). https://doi.org/10.3389/fmars.2019.00502

Bopp, L., Le Quéré, C., Heimann, M., Manning, A. C., & Monfray, P. (2002). Climate-induced oceanic oxygen fluxes: Implications for the contemporary carbon budget. *Global Biogeochemical Cycles*, *16*(2), 6-1–6-13. https://doi.org/10.1029/2001GB001445

Brown, P. J., Bakker, D. C. E., Schuster, U., & Watson, A. J. (2010). Anthropogenic carbon accumulation in the subtropical North Atlantic. *Journal of Geophysical Research*, *115*(C4), C04016. https://doi.org/10.1029/2008JC005043

Bryden, H. L., King, B. A., McCarthy, G. D., & McDonagh, E. L. (2014). Impact of a 30% reduction in Atlantic meridional overturning during 2009/2010. *Ocean Science*, *10*(4), 683–691. https://doi.org/10.5194/os-10-683-2014

Carpenter, E. J., & Capone, D. G. (2013). *Nitrogen in the marine environment*. Elsevier.

Carroll, D., Menemenlis, D., Adkins, J. F., Bowman, K. W., Brix, H., Dutkiewicz, S., et al (2020). The ECCO-Darwin data-assimilative global ocean biogeochemistry model: Estimates of seasonal to multidecadal surface ocean pCO_2 and air-sea CO_2 flux. *Journal of Advances in Modeling Earth Systems*, *12*(10), e2019MS001888. https://doi.org/10.1029/2019MS001888

Chaudhuri, A. H., Gangopadhyay, A., & Bisagni, J. J. (2011). Contrasting response of the eastern and western north atlantic circulation to an episodic climate event*. *Journal of Physical Oceanography*, *41*(9), 1630–1638. https://doi.org/10.1175/2011jpo4512.1

Cianca, A., Helmke, P., Mouriño, B., Rueda, M. J., Llinás, O., & Neuer, S. (2007). Decadal analysis of hydrography and in situ nutrient budgets in the western and eastern North Atlantic subtropical gyre. *Journal of Geophysical Research*, *112*(C7). https://doi.org/10.1029/2006JC003788

Culberson, C. H. (1991). *WOCE operations manual (WHP operations and methods), WHPO 91/1*. Woods Hole Oceanogr Inst, Woods Hole, MA.

Cunningham, S. A., Roberts, C. D., Frajka-Williams, E., Johns, W. E., Hobbs, W., Palmer, M. D., et al. (2013). Atlantic Meridional Overturning Circulation slowdown cooled the subtropical ocean. *Geophysical Research Letters*, *40*(23), 6202–6207. https://doi.org/10.1002/2013GL058464

Daniault, N., Mercier, H., Lherminier, P., Sarafanov, A., Falina, A., Zunino, P., et al. (2016). The northern North Atlantic Ocean mean circulation in the early 21st century. *Progress in Oceanography*, *146*, 142–158. https://doi.org/10.1016/j.pocean.2016.06.007. https://doi.org/10.1016/j.pocean.2016.06.007

Dave, A. C., Barton, A. D., Lozier, M. S., & McKinley, G. A. (2015). What drives seasonal change in oligotrophic area in the subtropical North Atlantic? *Journal of Geophysical Research: Oceans*, *120*(6), 3958–3969. https://doi.org/10.1002/2015JC010787

Dee, D. P., Uppala, S. M., Simmons, A. J., Berrisford, P., Poli, P., Kobayashi, S., et al (2011). The ERA-Interim reanalysis: Configuration and performance of the data assimilation system. *Quarterly Journal of the Royal Meteorological Society*, *137*(656), 553–597. https://doi.org/10.1002/qj.828

Desbruyères, D., Thierry, V., & Mercier, H. (2013). Simulated decadal variability of the meridional overturning circulation across the A25-Ovide section. *Journal of Geophysical Research: Oceans*, *118*(1), 462–475. https://doi.org/10.1029/2012JC008342

DeVries, T., Holzer, M., & Primeau, F. (2017). Recent increase in oceanic carbon uptake driven by weaker upper-ocean overturning. *Nature*, *542*(7640), 215–218. https://doi.org/10.1038/nature21068

Duce, R. A., LaRoche, J., Altieri, K., Arrigo, K. R., Baker, A. R., Capone, D. G., et al. (2008). Impacts of atmospheric anthropogenic nitrogen on the open ocean. *Science*, *320*(5878), 893–897. https://doi.org/10.1126/science.1150369

Emerson, S., Mecking, S., & Abell, J. (2001). The biological pump in the subtropical North Pacific Ocean: Nutrient sources, Redfield ratios, and recent changes. *Global Biogeochemical Cycles*, *15*(3), 535–554. https://doi.org/10.1029/2000GB001320

Falkowski, P. G., Barber, R. T., & Smetacek, V. (1998). Biogeochemical controls and feedbacks on ocean primary production. *Science*, *281*(5374), 200–206. https://doi.org/10.1126/science.281.5374.200

Fontela, M., García-Ibáñez, M. I., Hansell, D. A., Mercier, H., & Pérez, F. F. (2016). Dissolved organic carbon in the north Atlantic meridional overturning circulation. *Scientific Reports*, *6*(26931). https://doi.org/10.1038/srep26931

Fontela, M., Mercier, H., & Pérez, F. F. (2019). Long-term integrated biogeochemical budget driven by circulation in the eastern subpolar North Atlantic. *Progress in Oceanography*, *173*, 51–65. https://doi.org/10.1016/j.pocean.2019.02.004

Fratantoni, P. S., & McCartney, M. S. (2010). Freshwater export from the Labrador Current to the North Atlantic Current at the tail of the grand banks of newfoundland. *Deep Sea Research Part I: Oceanographic Research Papers*, *57*(2), 258–283. https://doi.org/10.1016/j.dsr.2009.11.006

Fröb, F., Olsen, A., Våge, K., Moore, G. W. K., Yashayaev, I., Jeansson, E., & Rajasakaren, B. (2016). Irminger Sea deep convection injects oxygen and anthropogenic carbon to the ocean interior. *Nature Communications*, *7*(13244). https://doi.org/10.1038/ncomms13244

Galbraith, E. D., Gnanadesikan, A., Dunne, J. P., & Hiscock, M. R. (2010). Regional impacts of iron-light colimitation in a global biogeochemical model. *Biogeosciences*, *7*(3), 1043–1064. https://doi.org/10.5194/bg-7-1043-2010

Ganachaud, A., & Wunsch, C. (2002). Oceanic nutrient and oxygen transports and bounds on export production during the World Ocean circulation experiment. *Global Biogeochemical Cycles*, *16*(4), 5-1–5-14. https://doi.org/10.1029/2000GB001333

García, H., Boyer, T. P., Levitus, S., Locarnini, R. A., & Antonov, J. (2005). On the variability of dissolved oxygen and apparent oxygen utilization content for the upper world ocean: 1955 to 1998. *Geophysical Research Letters*, *32*(9), L09604. https://doi.org/10.1029/2004GL022286

García, H., Cruzado, A., Gordon, L., & Escanez, J. (1998). Decadal-scale chemical variability in the subtropical North Atlantic deduced from nutrient and oxygen data. *Journal of Geophysical Research*, *103*(C2), 2817–2830. https://doi.org/10.1029/97JC03037

García-Ibáñez, M. I., Pardo, P. C., Carracedo, L. I., Mercier, H., Lherminier, P., Ríos, A. F., & Pérez, F. F. (2015). Structure, transports and transformations of the water masses in the Atlantic Subpolar gyre. *Progress in Oceanography*, *135*, 18–36. https://doi.org/10.1016/j.pocean.2015.03.009

Gruber, N., Clement, D., Carter, B. R., Feely, R. A., van Heuven, S., Hoppema, M., et al. (2019). The oceanic sink for anthropogenic CO2from 1994 to 2007. *Science*, *363*(6432), 1193–1199. https://doi.org/10.1126/science.aau5153

Gruber, N., Gloor, M., Fan, S.-M., & Sarmiento, J. L. (2001). Air-sea flux of oxygen estimated from bulk data: Implications for the marine and atmospheric oxygen cycles. *Global Biogeochemical Cycles*, *15*(4), 783–803. https://doi.org/10.1029/2000GB001302

Gruber, N., & Sarmiento, J. L. (1997). Global patterns of marine nitrogen fixation and denitrification. *Global Biogeochemical Cycles*, *11*(2), 235–266. https://doi.org/10.1029/97GB00077

Guallart, E. F., Schuster, U., Fajar, N. M., Legge, O., Brown, P., Pelejero, C., et al. (2015). Trends in anthropogenic CO2 in water masses of the Subtropical North Atlantic Ocean. *Progress in Oceanography*, *131*, 21–32. https://doi.org/10.1016/j.pocean.2014.11.006

Hansell, D. A., Carlson, C., Repeta, D., & Schlitzer, R. (2009). Dissolved organic matter in the ocean: A controversy stimulates new insights. *Oceanography*, *22*(4), 202–211. https://doi.org/10.5670/oceanog.2009.109

Hawkings, J. R., Wadham, J. L., Benning, L. G., Hendry, K. R., Tranter, M., Tedstone, A., et al (2017). Ice sheets as a missing source of silica to the polar oceans. *Nature Communications*, *8*(14198). https://doi.org/10.1038/ncomms14198

Heinze, C., Meyer, S., Goris, N., Anderson, L., Steinfeldt, R., Chang, N., et al. (2015). The ocean carbon sink - impacts, vulnerabilities and challenges. *Earth System Dynamics*, *6*(1), 327–358. https://doi.org/10.5194/esd-6-327-2015

Henson, S. A., Painter, S. C., Penny Holliday, N., Stinchcombe, M. C., & Giering, S. L. C. (2013). Unusual subpolar North Atlantic phytoplankton bloom in 2010: Volcanic fertilization or North Atlantic oscillation? *Journal of Geophysical Research: Oceans*, *118*(10), 4771–4780. https://doi.org/10.1002/jgrc.20363

Hernández-Guerra, A., Pelegrí, J. L., Fraile-Nuez, E., Benítez-Barrios, V., Emelianov, M., Pérez-Hernández, M. D., & Vélez-Belchí, P. (2014). Meridional overturning transports at 7.5N and 24.5N in the Atlantic Ocean during 1992-93 and 2010-11. *Progress in Oceanography*, *128*, 98–114. https://doi.org/10.1016/j.pocean.2014.08.016

Hurrell, J. W., Kushnir, Y., Ottersen, G., & Visbeck, M. (2013). An overview of the north atlantic oscillation. *The North Atlantic Oscillation: Climatic Significance and Environmental Impact*. https://doi.org/10.1029/134GM01

IPCC (2019). *IPCC Special Report on the Ocean and Cryosphere in a Changing Climate* (In H.-O. Pörtner, D. C. Roberts, V. Masson-Delmotte, P. Zhai, M. Tignor, E. Poloczanska, K. Mintenbeck, A. Alegría, M. Nicolai, A. Okem, J. Petzold, B. Rama, N. M. Weyer (eds.)). In press

Ito, T., & Follows, M. J. (2005). Preformed phosphate, soft tissue pump and atmospheric CO2. *Journal of Marine Research*, *63*(4), 813–839. https://doi.org/10.1357/0022240054663231

Jickells, T. D., Buitenhuis, E., Altieri, K., Baker, A. R., Capone, D., Duce, R. A., et al (2017). A reevaluation of the magnitude and impacts of anthropogenic atmospheric nitrogen inputs on the ocean. *Global Biogeochemical Cycles*, *31*(2), 2016GB005586. https://doi.org/10.1002/2016GB005586

Khatiwala, S., Tanhua, T., Mikaloff Fletcher, S., Gerber, M., Doney, S. C., Graven, H. D., et al. (2013). Global ocean storage of anthropogenic carbon. *Biogeosciences*, *10*(4), 2169–2191. https://doi.org/10.5194/bg-10-2169-2013

Kirkwood, D. (1996). *Nutrients: Practical notes on their determination in sea water*. Copenhagen, Denmark: International Council for the Exploration of the Sea.

Kistler, R., Collins, W., Saha, S., White, G., Woollen, J., Kalnay, E., et al. (2001). The NCEP-NCAR 50-year reanalysis: Monthly means CD-ROM and documentation. *Bulletin of the American Meteorological Society*, *82*(2), 247–267. https://doi.org/10.1175/1520-0477(2001)082<0247

Langdon, C. (2010). *Determination of dissolved oxygen in seawater by Winkler titration using the amperometric technique*. https://doi.org/10.1017/cbo9781139198073. Retrieved from https://repository.oceanbestpractices.org/handle/11329/380

Lavín, A. M., Bryden, H. L., & Parrilla, G. (2003). Mechanisms of heat, freshwater, oxygen and nutrient transports and budgets at 24.5°N in the subtropical North Atlantic. *Deep Sea Research Part I: Oceanographic Research Papers*, *50*(9), 1099–1128. https://doi.org/10.1016/S0967-0637(03)00095-5

Letscher, R. T., Primeau, F., & Moore, J. K. (2016). Nutrient budgets in the subtropical ocean gyres dominated by lateral transport. *Nature Geoscience*, *9*(11), 815–819. https://doi.org/10.1038/ngeo2812

Lherminier, P., Mercier, H., Gourcuff, C., Alvarez, M., Bacon, S., & Kermabon, C. (2007). Transports across the 2002 Greenland-Portugal Ovide section and comparison with 1997. *Journal of Geophysical Research*, *112*(C7), C07003. https://doi.org/10.1029/2006jc003716

Lherminier, P., Mercier, H., Huck, T., Gourcuff, C., Perez, F. F., Morin, P., et al. (2010). The Atlantic Meridional Overturning Circulation and the subpolar gyre observed at the A25-OVIDE section in June 2002 and 2004. *Deep Sea Research Part I: Oceanographic Research Papers*, *57*(11), 1374–1391. https://doi.org/10.1016/j.dsr.2010.07.009

Loucaides, S., Van Cappellen, P., Roubeix, V., Moriceau, B., & Ragueneau, O. (2012). Controls on the recycling and preservation of biogenic silica from biomineralization to burial. *Siliconindia*, *4*(1), 7–22. https://doi.org/10.1007/s12633-011-9092-9

Martel, F., & Wunsch, C. (1993). The North Atlantic Circulation in the Early 1980s-An Estimate from Inversion of a Finite-Difference Model. *Journal of Physical Oceanography*, *23*(5), 898–924. https://doi.org/10.1175/1520-0485(1993)023<0898:TNACIT>2.0.CO;2

Matear, R. J., & Hirst, A. C. (2003). Long-term changes in dissolved oxygen concentrations in the ocean caused by protracted global warming. *Global Biogeochemical Cycles*, *17*(4), 1125. https://doi.org/10.1029/2002GB001997

Maze, G., Mercier, H., Thierry, V., Memery, L., Morin, P., & Perez, F. F. (2012). Mass, nutrient and oxygen budgets for the northeastern Atlantic Ocean. *Biogeosciences*, *9*(10), 4099–4113. https://doi.org/10.5194/bg-9-4099-2012

McCarthy, G. D., Frajka-Williams, E., Johns, W. E., Baringer, M. O., Meinen, C. S., Bryden, H. L., et al (2012). Observed interannual variability of the Atlantic meridional overturning circulation at 26.5°N: Interannual variability of the MOC. *Geophysical Research Letters*, *39*(19). https://doi.org/10.1029/2012GL052933

McCarthy, G. D., Smeed, D. A., Johns, W. E., Frajka-Williams, E., Moat, B. I., Rayner, D., et al. (2015). Measuring the Atlantic Meridional Overturning Circulation at 26°N. *Progress in Oceanography*, *130*, 91–111. https://doi.org/10.1016/j.pocean.2014.10.006

McDonagh, E. L., King, B. A., Bryden, H. L., Courtois, P., Szuts, Z., Baringer, M., et al. (2015). Continuous estimate of atlantic oceanic freshwater flux at 26.5°N. *Journal of Climate*, *28*(22), 8888–8906. https://doi.org/10.1175/JCLI-D-14-00519.1

Meinen, C. S., Baringer, M. O., & Garcia, R. F. (2010). Florida Current transport variability: An analysis of annual and longer-period signals. *Deep Sea Research Part I: Oceanographic Research Papers*, *57*(7), 835–846. https://doi.org/10.1016/j.dsr.2010.04.001

Mercier, H. (1986). Determining the general circulation of the ocean: A nonlinear inverse problem. *Journal of Geophysical Research*, *91*(C4), 5103–5109. https://doi.org/10.1029/jc091ic04p05103

Mercier, H., Lherminier, P., Sarafanov, A., Gaillard, F., Daniault, N., Desbruyères, D., et al. (2015). Variability of the meridional overturning circulation at the Greenland-Portugal OVIDE section from 1993 to 2010. *Progress in Oceanography*, *132*, 250–261. https://doi.org/10.1016/j.pocean.2013.11.001

Michaels, A. F., Olson, D., Sarmiento, J. L., Ammerman, J. W., Fanning, K., Jahnke, R., et al. (1996). Inputs, losses and transformations of nitrogen and phosphorus in the pelagic North Atlantic Ocean. *Biogeochemistry*, *35*(1), 181–226. https://doi.org/10.1007/BF02179827

Moore, C. M., Mills, M. M., Arrigo, K. R., Berman-Frank, I., Bopp, L., Boyd, P. W., et al. (2013). Processes and patterns of oceanic nutrient limitation. *Nature Geoscience*, *6*(9), 701–710. https://doi.org/10.1038/ngeo1765

Olsen, A., Lange, N., Key, R. M., Tanhua, T., Álvarez, M., Becker, S., et al. (2019). GLODAPv2.2019 – an update of GLODAPv2. *Earth System Science Data*, *11*(3), 1437–1461. https://doi.org/10.5194/essd-11-1437-2019

Osborn, T. J. (2011). Winter 2009/2010 temperatures and a record-breaking North Atlantic Oscillation index. *Weather*, *66*(1), 19–21. https://doi.org/10.1002/wea.660

Oschlies, A. (2001). NAO-induced long-term changes in nutrient supply to the surface waters of the North Atlantic. *Geophysical Research Letters*, *28*(9), 1751–1754. https://doi.org/10.1029/2000GL012328

Palter, J. B., Lozier, M. S., & Barber, R. T. (2005). The effect of advection on the nutrient reservoir in the North Atlantic subtropical gyre. *Nature*, *437*(7059), 687–692. https://doi.org/10.1038/nature03969

Palter, J. B., Lozier, M. S., Sarmiento, J. L., & Williams, R. G. (2011). The supply of excess phosphate across the Gulf Stream and the maintenance of subtropical nitrogen fixation. *Global Biogeochemical Cycles*, *25*(4). https://doi.org/10.1029/2010GB003955

Pelegrí, J. L., & Csanady, G. T. (1991). Nutrient transport and mixing in the Gulf Stream. *Journal of Geophysical Research*, *96*(C2), 2577–2583. https://doi.org/10.1029/90JC02535

Pelegrí, J. L., Marrero-Díaz, A., & Ratsimandresy, A. W. (2006). Nutrient irrigation of the North Atlantic. *Progress in Oceanography*, *70*(2–4), 366–406. https://doi.org/10.1016/j.pocean.2006.03.018

Pérez, F. F., Gilcoto, M., & Ríos, A. F. (2003). Large and mesoscale variability of the water masses and the deep chlorophyll maximum in the Azores Front. *Journal of Geophysical Research*, *1083215*(C7). https://doi.org/10.1029/2000JC000360

Pommier, J., Gosselin, M., & Michel, C. (2009). Size-fractionated phytoplankton production and biomass during the decline of the northwest Atlantic spring bloom. *Journal of Plankton Research*, *31*(4), 429–446. https://doi.org/10.1093/plankt/fbn127

Ragueneau, O., Gallinari, M., Corrin, L., Grandel, S., Hall, P., Hauvespre, A., et al. (2001). The benthic silica cycle in the Northeast Atlantic: Annual mass balance, seasonality, and importance of non-steady-state processes for the early diagenesis of biogenic opal in deep-sea sediments. *Progress in Oceanography*, *50*(1), 171–200. https://doi.org/10.1016/S0079-6611(01)00053-2

Ragueneau, O., Tréguer, P., Leynaert, A., Anderson, R. F., Brzezinski, M. A., DeMaster, D. J., et al. (2000). A review of the Si cycle in the modern ocean: Recent progress and missing gaps in the application of biogenic opal as a paleoproductivity proxy. *Global and Planetary Change*, *26*(4), 317–365. https://doi.org/10.1016/S0921-8181(00)00052-7

Reygondeau, G., Longhurst, A., Martinez, E., Beaugrand, G., Antoine, D., & Maury, O. (2013). Dynamic biogeochemical provinces in the global ocean. *Global Biogeochemical Cycles*, *27*(4), 1046–1058. https://doi.org/10.1002/gbc.20089

Riebesell, U., Körtzinger, A., & Oschlies, A. (2009). Sensitivities of marine carbon fluxes to ocean change. *Proceedings of the National Academy of Sciences*, *106*(49), 20602–20609. https://doi.org/10.1073/pnas.0813291106

Rintoul, S. R., & Wunsch, C. (1991). Mass, heat, oxygen and nutrient fluxes and budgets in the North Atlantic Ocean. *Deep-Sea Research Part A. Oceanographic Research Papers*, *38*, S355–S377. https://doi.org/10.1016/S0198-0149(12)80017-3

Sarafanov, A. (2009). On the effect of the North Atlantic Oscillation on temperature and salinity of the subpolar North Atlantic intermediate and deep waters. *ICES Journal of Marine Science: Journal Du Conseil*, *66*(7), 1448–1454. https://doi.org/10.1093/icesjms/fsp094

Schlitzer, R. (1988). Modeling the nutrient and carbon cycles of the North Atlantic: 1. Circulation, mixing coefficients, and heat fluxes. *Journal of Geophysical Research*, *93*(C9), 10699–10723. https://doi.org/10.1029/JC093iC09p10699

Schmittner, A. (2005). Decline of the marine ecosystem caused by a reduction in the Atlantic overturning circulation. *Nature*, *434*(7033), 628–633. https://doi.org/10.1038/nature03476

Segschneider, J., & Bendtsen, J. (2013). Temperature-dependent remineralization in a warming ocean increases surface pCO_2 through changes in marine ecosystem composition. *Global Biogeochemical Cycles*, *27*(4), 2013GB004684. https://doi.org/10.1002/2013GB004684

Seitzinger, S. P., Mayorga, E., Bouwman, A. F., Kroeze, C., Beusen, A. H. W., Billen, G., et al. (2010). Global river nutrient export: A scenario analysis of past and future trends. *Global Biogeochemical Cycles*, *24*(4). https://doi.org/10.1029/2009GB003587

Siedler, G., Church, J., Gould, J., & Gould, W. J. (2001). *Ocean circulation and climate: Observing and modeling the global ocean*. Academic Press.

Smeed, D., Josey, S. A., Beaulieu, C., Johns, W. E., Moat, B. I., Frajka-Williams, E., et al (2018). The North Atlantic Ocean is in a state of reduced overturning. *Geophysical Research Letters*, *45*(3), 2017GL076350. https://doi.org/10.1002/2017GL076350

Smeed, D., McCarthy, G. D., Cunningham, S. A., Frajka-Williams, E., Rayner, D., Johns, W. E., et al. (2014). Observed decline of the Atlantic meridional overturning circulation 2004–2012. *Ocean Science*, *10*(1), 29–38. https://doi.org/10.5194/os-10-29-2014

Smeed, D., Moat, B. I., Rayner, D., Johns, W. E., Baringer, M. O., Volkov, D. L., & Frajka-Williams, E. (2019). Atlantic meridional overturning circulation observed by the RAPID-MOCHA-WBTS array at 26N from 2004 to 2018. *British Oceanographic Data Centre*. https://doi.org/10.5285/c72s

Srokosz, M. A., & Bryden, H. L. (2015). Observing the Atlantic Meridional Overturning Circulation yields a decade of inevitable surprises. *Science*, *348*(6241), 1255575. https://doi.org/10.1126/science.1255575

Stendardo, I., & Gruber, N. (2012). Oxygen trends over five decades in the North Atlantic. *Journal of Geophysical Research*, *117*(C11). https://doi.org/10.1029/2012JC007909

Stepanov, V. N., & Haines, K. (2014). Mechanisms of Atlantic Meridional Overturning Circulation variability simulated by the NEMO model. *Ocean Science*, *10*(4), 645–656. https://doi.org/10.5194/os-10-645-2014

Stock, C. A., Dunne, J. P., & John, J. G. (2014). Global-scale carbon and energy flows through the marine planktonic food web: An analysis with a coupled physical-biological model. *Progress in Oceanography*, *120*, 1–28. https://doi.org/10.1016/j.pocean.2013.07.001

Stocker, T. F., Qin, D., Plattner, G.-K., Tignor, M., Allen, S. K., Boschung, J., et al (2013). *Climate change 2013: The physical science basis. Contribution of working group I to the fifth assessment report of the intergovernmental panel on climate change*. Cambridge, United Kingdom: Cambridge University Press. Retrieved from. https://doi.org/10.1017/CBO9781107415324

Stramma, L., Johnson, G. C., Sprintall, J., & Mohrholz, V. (2008). Expanding oxygen-minimum zones in the tropical oceans. *Science*, *320*(5876), 655–658. https://doi.org/10.1126/science.1153847

Stramma, L., Schmidtko, S., Levin, L. A., & Johnson, G. C. (2010). Ocean oxygen minima expansions and their biological impacts. *Deep Sea Research Part I: Oceanographic Research Papers*, *57*(4), 587–595. https://doi.org/10.1016/j.dsr.2010.01.005

Sutton, R. T., McCarthy, G. D., Robson, J., Sinha, B., Archibald, A. T., & Gray, L. J. (2017). Atlantic multidecadal variability and the U.K. ACSIS program. *Bulletin of the American Meteorological Society*, *99*(2), 415–425. https://doi.org/10.1175/BAMS-D-16-0266.1

Takahashi, T., Sutherland, S. C., Wanninkhof, R., Sweeney, C., Feely, R. A., Chipman, D. W., et al. (2009). Climatological mean and decadal change in surface ocean pCO2, and net sea-air CO2 flux over the global oceans. *Deep Sea Research Part II: Topical Studies in Oceanography*, *56*(8–10), 554–577. https://doi.org/10.1016/j.dsr2.2008.12.009

Taws, S. L., Marsh, R., Wells, N. C., & Hirschi, J. (2011). Re-emerging ocean temperature anomalies in late-2010 associated with a repeat negative NAO. *Geophysical Research Letters*, *38*(20), a–n. https://doi.org/10.1029/2011GL048978

Torres-Valdés, S., Tsubouchi, T., Bacon, S., Naveira-Garabato, A. C., Sanders, R., McLaughlin, F. A., et al. (2013). Export of nutrients from the Arctic Ocean. *Journal of Geophysical Research: Oceans*, *118*(4), 1625–1644. https://doi.org/10.1002/jgrc.20063

Tréguer, P., & De La Rocha, C. L. (2013). The world ocean silica cycle. *Annual Review of Marine Science*, *5*(1), 477–501. https://doi.org/10.1146/annurev-marine-121211-172346

Tréguer, P., Nelson, D. M., Van Bennekom, A. J., DeMaster, A. J., Leynaert, A., & Quéguiner, B. (1995). The silica balance in the world ocean: A reestimate. *Science*, *268*(5209), 375–379. https://doi.org/10.1126/science.268.5209.375

Watson, A. J., Schuster, U., Bakker, D. C. E., Bates, N. R., Corbiere, A., Gonzalez-Davila, M., et al. (2009). Tracking the Variable North Atlantic Sink for Atmospheric CO2. *Science*, *326*, 1391–1393. https://doi.org/10.1126/science.1177394

Williams, R. G., & Follows, M. J. (1998). The Ekman transfer of nutrients and maintenance of new production over the North Atlantic. *Deep Sea Research Part I: Oceanographic Research Papers*, *45*(2), 461–489. https://doi.org/10.1016/S0967-0637(97)00094-0

Williams, R. G., & Follows, M. J. (2003). Physical Transport of Nutrients and the Maintenance of Biological Production. In *Ocean biogeochemistry* (pp. 19–51). Berlin, Heidelberg: Springer. https://doi.org/10.1007/978-3-642-55844-3_3

Williams, R. G., McDonagh, E., Roussenov, V. M., Torres-Valdes, S., King, B., Sanders, R., & Hansell, D. A. (2011). Nutrient streams in the North Atlantic: Advective pathways of inorganic and dissolved organic nutrients. *Global Biogeochemical Cycles*, *25*(4). https://doi.org/10.1029/2010GB003853

Williams, R. G., McLaren, A. J., & Follows, M. J. (2000). Estimating the convective supply of nitrate and implied variability in export production over the North Atlantic. *Global Biogeochemical Cycles*, *14*(4), 1299–1313. https://doi.org/10.1029/2000GB001260

Williams, R. G., Roussenov, V., & Follows, M. J. (2006). Nutrient streams and their induction into the mixed layer. *Global Biogeochemical Cycles*, *20*. https://doi.org/10.1029/2005GB002586

Yool, A., Popova, E. E., & Anderson, T. R. (2013). MEDUSA-2.0: An intermediate complexity biogeochemical model of the marine carbon cycle for climate change and ocean acidification studies. *Geoscientific Model Development*, *6*(5), 1767–1811. https://doi.org/10.5194/gmd-6-1767-2013

References From the Supporting Information

Curry, B., Lee, C. M., Petrie, B., Moritz, R. E., & Kwok, R. (2014). Multiyear Volume, Liquid Freshwater, and Sea Ice Transports through Davis Strait, 2004-10*. *Journal of Physical Oceanography*, *44*(4), 1244–1266. https://doi.org/10.1175/JPO-D-13-0177.1

Dürr, H. H., Meybeck, M., Hartmann, J., Laruelle, G. G., & Roubeix, V. (2011). Global spatial distribution of natural riverine silica inputs to the coastal zone. *Biogeosciences*, *8*(3), 597–620. https://doi.org/10.5194/bg-8-597-2011

Ganachaud, A. (2003). Error budget of inverse box models: The North Atlantic. *Journal of Atmospheric and Oceanic Technology*, *20*(11), 1641–1655. https://doi.org/10.1175/1520-0426(2003)020<1641:eboibm>2.0.co;2

Hansell, D. A., & Follows, M. J. (2008). Nitrogen in the Atlantic Ocean. In *Nitrogen in the marine environment* (2nd ed.; pp. 597–630). San Diego: Academic Press. https://doi.org/10.1016/B978-0-12-372522-6.00013-X

Holliday, N. P., Bacon, S., Cunningham, S. A., Gary, S. F., Karstensen, J., King, B. A., et al. (2018). Subpolar North Atlantic overturning and gyre-scale circulation in the summers of 2014 and 2016. *Journal of Geophysical Research: Oceans*, *123*(7), 4538–4559. https://doi.org/10.1029/2018JC013841

Huertas, I. E., Ríos, A. F., García-Lafuente, J., Navarro, G., Makaoui, A., Sánchez-Román, A., et al (2012). Atlantic forcing of the Mediterranean oligotrophy. *Global Biogeochemical Cycles*, *26*(2). https://doi.org/10.1029/2011GB004167

Kanzow, T., Cunningham, S. A., Johns, W. E., Hirschi, J. J.-M., Marotzke, J., Baringer, M. O., et al. (2010). Seasonal variability of the atlantic meridional overturning circulation at 26.5°N. *Journal of Climate*, *23*(21), 5678–5698. https://doi.org/10.1175/2010JCLI3389.1

Letscher, R. T., Hansell, D. A., Carlson, C. A., Lumpkin, R., & Knapp, A. N. (2013). Dissolved organic nitrogen in the global surface ocean: Distribution and fate. *Global Biogeochemical Cycles*, *27*(1), 141–153. https://doi.org/10.1029/2012GB004449

Mahaffey, C., Williams, R. G., Wolff, G. A., & Anderson, W. T. (2004). Physical supply of nitrogen to phytoplankton in the Atlantic Ocean. *Global Biogeochemical Cycles*, *18*(1). https://doi.org/10.1029/2003GB002129

Mahowald, N., Jickells, T. D., Baker, A. R., Artaxo, P., Benitez-Nelson, C. R., Bergametti, G., et al. (2008). Global distribution of atmospheric phosphorus sources, concentrations and deposition rates, and anthropogenic impacts. *Global Biogeochemical Cycles*, *22*(4). https://doi.org/10.1029/2008GB003240

Mather, R. L., Reynolds, S. E., Wolff, G. A., Williams, R. G., Torres-Valdes, S., Woodward, E. M. S., et al. (2008). Phosphorus cycling in the North and South Atlantic Ocean subtropical gyres. *Nature Geoscience*, *1*(7), 439–443. https://doi.org/10.1038/ngeo232

Mayorga, E., Seitzinger, S. P., Harrison, J. A., Dumont, E., Beusen, A. H. W., Bouwman, A. F., et al. (2010). Global Nutrient Export from WaterSheds 2 (NEWS 2): Model development and implementation. *Environmental Modelling & Software*, *25*(7), 837–853. https://doi.org/10.1016/j.envsoft.2010.01.007

Peucker-Ehrenbrink, B. (2009). Land2Sea database of river drainage basin sizes, annual water discharges, and suspended sediment fluxes. *Geochemistry, Geophysics, Geosystems*, *10*(6). https://doi.org/10.1029/2008GC002356

Racapé, V., Zunino, P., Mercier, H., Lherminier, P., Bopp, L., Pérèz, F. F., & Gehlen, M. (2018). Transport and storage of anthropogenic C in the North Atlantic Subpolar Ocean. *Biogeosciences*, *15*(14), 4661–4682. https://doi.org/10.5194/bg-15-4661-2018

Reynolds, S., Mahaffey, C., Roussenov, V., & Williams, R. G. (2014). Evidence for production and lateral transport of dissolved organic phosphorus in the eastern subtropical North Atlantic. *Global Biogeochemical Cycles*, *28*(8), 805–824. https://doi.org/10.1002/2013GB004801

Roussenov, V., Williams, R. G., Mahaffey, C., & Wolff, G. A. (2006). Does the transport of dissolved organic nutrients affect export production in the Atlantic Ocean? *Global Biogeochemical Cycles*, *20*(3). https://doi.org/10.1029/2005GB002510

Serreze, M. C., Barrett, A. P., Slater, A. G., Woodgate, R. A., Aagaard, K., Lammers, R. B., et al (2006). The large-scale freshwater cycle of the Arctic. *Journal of Geophysical Research*, *111*(C11). https://doi.org/10.1029/2005JC003424

Sharples, J., Middelburg, J. J., Fennel, K., & Jickells, T. D. (2016). What proportion of riverine nutrients reaches the open ocean? *Global Biogeochemical Cycles*, *31*(1), 2016GB005483. https://doi.org/10.1002/2016GB005483

Singh, A., Lomas, M. W., & Bates, N. R. (2013). Revisiting N2 fixation in the North Atlantic Ocean: Significance of deviations from the Redfield Ratio, atmospheric deposition and climate variability. *Deep Sea Research Part II: Topical Studies in Oceanography*, *93*, 148–158. https://doi.org/10.1016/j.dsr2.2013.04.008

Talley, L. D., Pickard, G. L., Emery, W. J., & Swift, J. H. (2007). *Descriptive physical oceanography, sixth edition: An introduction* (6th ed.). Academic Press.

Torres-Valdés, S., Roussenov, V. M., Sanders, R., Reynolds, S., Pan, X., Mather, R., et al (2009). Distribution of dissolved organic nutrients and their effect on export production over the Atlantic Ocean. *Global Biogeochemical Cycles*, *23*(4). https://doi.org/10.1029/2008GB003389

Treguier, A. M., Gourcuff, C., Lherminier, P., Mercier, H., Barnier, B., Madec, G., et al. (2006). Internal and forced variability along a section between Greenland and Portugal in the CLIPPER Atlantic model. *Ocean Dynamics*, *56*(5–6), 568–580. https://doi.org/10.1007/s10236-006-0069-y

Tsubouchi, T., Bacon, S., Naveira Garabato, A. C., Aksenov, Y., Laxon, S. W., Fahrbach, E., et al. (2012). The Arctic Ocean in summer: A quasi-synoptic inverse estimate of boundary fluxes and water mass transformation. *Journal of Geophysical Research*, *117*(C1), C01024. https://doi.org/10.1029/2011JC007174

Woodgate, R. A., & Aagaard, K. (2005). Revising the Bering Strait freshwater flux into the Arctic Ocean. *Geophysical Research Letters*, *32*(2). https://doi.org/10.1029/2004GL021747

Woodgate, R. A., Aagaard, K., & Weingartner, T. J. (2005). Monthly temperature, salinity, and transport variability of the Bering Strait through flow. *Geophysical Research Letters*, *32*(4). https://doi.org/10.1029/2004GL021880

Yang, S., & Gruber, N. (2016). The anthropogenic perturbation of the marine nitrogen cycle by atmospheric deposition: Nitrogen cycle feedbacks and the 15 N Haber-Bosch effect. *Global Biogeochemical Cycles*, *30*(10), 1418–1440. https://doi.org/10.1002/2016GB005421

Zunino, P., Garcia-Ibañez, M. I., Lherminier, P., Mercier, H., Ríos, A. F., & Pérez, F. F. (2014). Variability of the transport of anthropogenic CO2 at the Greenland-Portugal OVIDE section: Controlling mechanisms. *Biogeosciences*, *11*(8), 2375–2389. https://doi.org/10.5194/bg-11-2375-2014

Zunino, P., Pérez, F. F., Fajar, N. M., Guallart, E. F., Ríos, A. F., Pelegrí, J. L., & Hernández-Guerra, A. (2015). Transports and budgets of anthropogenic CO_2 in the tropical North Atlantic in 1992–1993 and 2010–2011. *Global Biogeochemical Cycles*, *29*(7), 2014GB005075. https://doi.org/10.1002/2014GB005075